gigantea Suppresses *immutans* Variegation by Interactions with Cytokinin and Gibberellin Signaling Pathways[1][W][OPEN]

Aarthi Putarjunan and Steve Rodermel*

Department of Genetics, Development, and Cell Biology, Iowa State University, Ames, Iowa 50011

The *immutans* (*im*) variegation mutant of Arabidopsis (*Arabidopsis thaliana*) is an ideal model to gain insight into factors that control chloroplast biogenesis. *im* defines the gene for PTOX, a plastoquinol terminal oxidase that participates in the control of thylakoid redox. Here, we report that the *im* defect can be suppressed during the late stages of plant development by *gigantea* (*gi2*), which defines the gene for GI, a central component of the circadian clock that plays a poorly understood role in diverse plant developmental processes. *imgi2* mutants are late flowering and display other well-known phenotypes associated with *gi2*, such as starch accumulation and resistance to oxidative stress. We show that the restoration of chloroplast biogenesis in *imgi2* is caused by a development-specific derepression of cytokinin signaling that involves cross talk with signaling pathways mediated by gibberellin (GA) and SPINDLY (SPY), a GA response inhibitor. Suppression of the plastid defect in *imgi2* is likely caused by a relaxation of excitation pressures in developing plastids by factors contributed by *gi2*, including enhanced rates of photosynthesis and increased resistance to oxidative stress. Interestingly, the suppression phenotype of *imgi* can be mimicked by crossing *im* with the starch accumulation mutant, *starch excess1* (*sex1*), perhaps because *sex1* utilizes pathways similar to *gi*. We conclude that our studies provide a direct genetic linkage between GI and chloroplast biogenesis, and we construct a model of interactions between signaling pathways mediated by *gi*, GA, SPY, cytokinins, and *sex1* that are required for chloroplast biogenesis.

The *immutans* (*im*) variegation mutant of Arabidopsis (*Arabidopsis thaliana*), first studied by Rédei and Röbbelen more than 50 years ago, is an ideal developmental system to gain insight into the poorly understood mechanisms of chloroplast biogenesis (Rédei, 1963, 1967; Röbbelen, 1968; Putarjunan et al., 2013). This process entails the differentiation of chloroplasts from proplastids in the leaf meristem or from etioplasts in illuminated dark-grown seedlings (Pogson and Albrecht, 2011). Green/white sectoring in all normally green organs of *im* is caused by a nuclear recessive gene, and cells in the mutant have a uniform *im/im* genotype (Rédei, 1963, 1967; Röbbelen 1968); all *im* alleles reported to date are null (Putarjunan et al., 2013). Whereas chloroplasts in the green sectors resemble those in the wild type with respect to pigment composition and morphology, plastids in the white sectors are vacuolated, lack lamellar structures, and accumulate phytoene, an early (colorless) C_{40} intermediate in the carotenoid biosynthetic pathway (Wetzel et al., 1994). Cloning of *IM* by map-based and transfer DNA-tagging methods revealed that the gene codes for a plastid membrane-localized plastoquinol oxidase (PTOX) that bears functional and structural similarity to the alternative oxidase class of mitochondrial inner membrane ubiquinol terminal oxidases (Carol et al., 1999; Wu et al., 1999).

It is now well established that PTOX functions as a terminal oxidase in the redox regulation of developing and mature thylakoids by transferring electrons from plastoquinol to molecular oxygen, forming water and plastoquinone (PQ; McDonald et al., 2011). In addition to linear electron transport, PTOX activity can be coupled to other processes that feed electrons to the PQ pool, including chlororespiration, cyclic electron flow around PSI, and the two desaturation steps of carotenoid biosynthesis catalyzed by phytoene desaturase and ζ-carotene desaturase (Albrecht et al., 1995; Peltier and Cournac, 2002; Okegawa et al., 2010; Putarjunan et al., 2013). It can also act as a safety valve to dissipate excess absorbed energy, thereby preventing the overreduction of photosynthetic electron carriers and protecting PSI and PSII from photoinhibition (McDonald et al., 2011; Foudree et al., 2012; Putarjunan et al., 2013). In the absence of PTOX, developing thylakoids become overreduced and phytoene accumulates, either because of a decreased supply of PQ available to phytoene desaturase and/or because electron transfer from phytoene to an overreduced PQ pool is not energetically

[1] This work was supported by the Chemical Sciences, Geosciences, and Biosciences Division, Office of Basic Energy Sciences, Office of Science, U.S. Department of Energy (grant no. DEFG02–94ER20147 to S.R.).

* Address correspondence to rodermel@iastate.edu.

The author responsible for distribution of materials integral to the findings presented in this article in accordance with the policy described in the Instructions for Authors (www.plantphysiol.org) is: Steve Rodermel (rodermel@iastate.edu).

[W] The online version of this article contains Web-only data.

[OPEN] Articles can be viewed online without a subscription.

www.plantphysiol.org/cgi/doi/10.1104/pp.114.250647

favorable (Shahbazi et al., 2007; Rosso et al., 2009). This blockage prevents the accumulation of downstream (photoprotective) carotenoids, generating photooxidized (white) plastids. The extent of photooxidation, and white sector formation, is promoted by growth under restrictive conditions of high light or low temperature (Rosso et al., 2009).

Our current working hypothesis of the mechanism of *im* variegation is based on the premise that white sector formation is positively correlated with excitation pressures (EPs; Rosso et al., 2009); EP is a relative measure of the reduction state of the first stable electron acceptor of PSII (Dietz et al., 1985; Hüner et al., 1998). According to the threshold hypothesis, above-threshold EPs predispose developing *im* plastids to photooxidation, while plastids with below-threshold EPs develop into normal chloroplasts (Wetzel et al., 1994; Putarjunan et al., 2013). The observation that *im* contains heteroplastidic cells (with normal and abnormal plastids) argues that chloroplast biogenesis is also plastid autonomous (Wetzel et al., 1994; i.e. that EPs vary from plastid to plastid in the developing leaf primordium). This variation is promoted by the unique location of each plastid in the developing leaf, which dictates that each plastid has a unique biochemistry. For instance, plastids are subjected to widely varying concentrations of photosynthetic substrates such as light and CO_2 that are present in steep gradients across the leaf lamina (Smith et al., 1997). A final assumption of our model is that the chaotic pattern of *im* variegation in the mature leaf is a reflection of the pattern of dicot leaf development: white plastids in cells of the leaf primordium give rise to clones of white plastids, cells, and sectors in the mature leaf, whereas chloroplasts in the developing primordium produce green cells and sectors.

We have turned to second-site suppressor analysis to identify genes that modify the *im* variegation phenotype as an approach to gain entrance into mechanisms of PTOX function, *im* variegation, and chloroplast biogenesis (Putarjunan et al., 2013). Our operating assumption is that suppressors can provide information about PTOX function and activity per se (e.g. interaction suppressors) as well as knowledge about factors and pathways that act early in chloroplast biogenesis but that might not be easily accessible by other means (bypass suppressors). In our search for *im* suppressors, we were intrigued by an observation of Rédei (1967) that vigorous vegetative growth of *im* could be obtained by crossing it with *gigantea* (*gi*), a late-flowering supervital mutant that had been recently isolated (Rédei, 1962). Unfortunately, Rédei (1967) did not describe the chloroplast phenotype of the *imgi* double mutants or their phenotype during development; the traits were assumed to act independently. However, it has since become apparent that supervitality is one of many strikingly diverse, and seemingly unrelated, phenotypes caused by *GI* deficiency. Others include alterations in period lengths of circadian rhythms (Park et al., 1999), resistance to paraquat (Kurepa et al., 1998a), impairment in phytochrome B signaling (Huq et al., 2000), enhanced accumulation of starch (Eimert et al., 1995) and anthocyanins (Kurepa et al., 1998b), elevated expression of detoxifying enzymes such as superoxide dismutase (SOD) and ascorbate peroxidase (APX) in the presence of paraquat (Cao et al., 2006), and increased sensitivity to freezing (Cao et al., 2007). *GI* was cloned nearly 40 years after Rédei's initial description of *gi* (Fowler et al., 1999), and molecular analyses since that time have revealed that *GI* acts as a scaffold protein for the assembly of complexes that mediate protein-protein stability/activity via the 26S proteasome (Kim et al., 2007; Sawa et al., 2007; Yu et al., 2008b). It also interacts with a number of components of the circadian clock-associated flowering pathway in Arabidopsis and plays an important role in photoperiodic flowering (Fowler et al., 1999; Park et al., 1999; Sawa and Kay, 2011).

We were prompted by the observations of Rédei (1967) to revisit *imgi* as a tool to understand PTOX function and mechanisms of chloroplast biogenesis. In this article, we show that *gi* suppresses *im* variegation during the late stages of plant development by generating all-green versus variegated newly emerging leaves. We demonstrate that this suppression occurs via interactions between *GI* and cytokinin-mediated signaling pathways and that these paths are integrated by the GA response inhibitor SPINDLY (SPY). These interactions are described in a model that we test, showing that a reduction in GA signaling late in *gi* development derepresses cytokinin signaling, which reprograms processes required for chloroplast differentiation. Importantly, these processes include an enhancement of photosynthetic rates and an elevated reactive oxygen species (ROS) scavenging capacity. We show that when *gi* is combined with *im* in the double mutant, these processes act in concert to relax EPs, thereby promoting the formation of photosynthetically competent chloroplasts and suppression of the *im* defect.

RESULTS

Variegation Is Suppressed in *imgi2* during Late Plant Development

To examine interactions between *im* and *gi*, double mutants were generated by crossing null alleles of *im* (*spotty*) and *gi* (*gi2*; Park et al., 1999; Wu et al., 1999); the genotypes of the double mutants were identified in the F2 generation by PCR amplification. *imgi2* plants have higher than normal leaf numbers and are late flowering (Fig. 1, A and B). This delay in the floral transition is similar to *gi2* but unlike *im* and the wild type. Whereas *imgi2* is variegated during early plant development, perhaps the most striking phenotype of *imgi2* is a suppression of variegation that occurs during late development, commencing approximately 9 weeks after germination. After this time, newly emerging

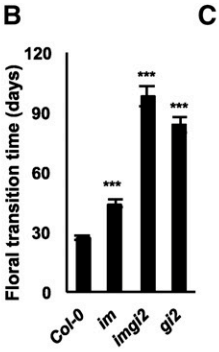

C

	Stage I (4 weeks)	Stage II (10 weeks)	Stage III (12 weeks)
Col-0	Vegetative (pre-flowering)	Reproductive	Senescent
im	Vegetative (pre-flowering) Variegated	Reproductive Variegated	Senescent Variegated
imgi2	Vegetative Variegated	Vegetative Less-variegated	Vegetative (pre-flowering) All-green
gi2	Vegetative	Vegetative (pre-flowering)	Reproductive

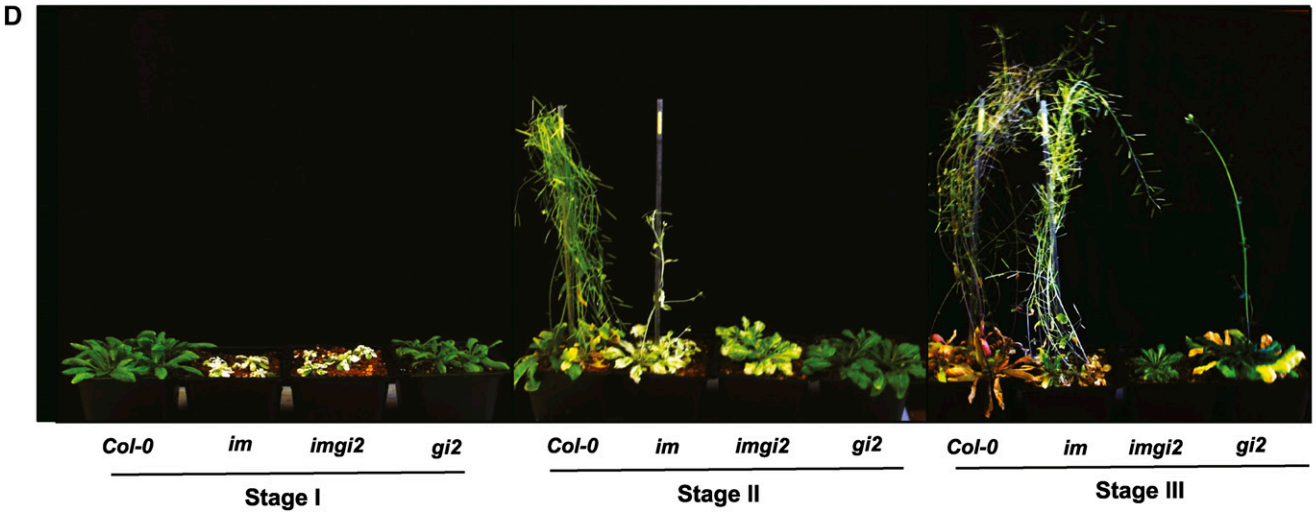

Figure 1. Growth stages of *imgi2*, *gi2*, *im*, and the wild type. A, *imgi2* rosettes at 9, 10, and 12 weeks after germination. Plants were grown at 22°C under conditions of continuous illumination (100 μmol m^{-2} s^{-1}). B, Time taken to achieve the floral transition in the wild type (Col-0), *im*, *imgi2*, and *gi2*. Values represent averages ± SE of five independent replicates relative to Col-0 (***$P < 0.001$). C, Summary table of developmental stages associated with Col-0, *im*, *imgi2*, and *gi2* at 4 weeks (stage I), 10 weeks (stage II), and 12 weeks (stage III) after germination. D, Representative Col-0, *im*, *imgi2*, and *gi2* plants examined at the three developmental stages.

leaves are all green. This suggests that *gi2* is able to suppress *im* variegation in a development-dependent manner.

Because valid interpretations of the experiments in this report rely on the ability to compare wild-type and mutant plants at the same stage of development (versus the same chronological age), it was necessary to obtain a global assessment of the developmental profiles of *imgi2*, the wild type (Columbia-0 [Col-0]), *im*, and *gi2*. These data are shown in Figure 1D and summarized in Figure 1C. For these experiments, we chose to examine plants at three time points after germination, designated stage I (4 weeks), stage II (10 weeks), and stage III (12 weeks). These times were selected because they correlate with the timing of the dramatic phenotypic changes in *imgi2* leaf coloration: emerging leaves are variegated during early vegetative development (stage I, until approximately 9 weeks), less variegated starting at about 10 weeks (stage II), and finally all green during late vegetative development (stage III, 12 weeks). Flowering commences 14 or so weeks after *imgi2* germination (Fig. 1B). The development of *gi2* proceeds in a manner similar to *imgi2*, with the exception that *gi2* begins to flower earlier (during stage III). Finally, *im* and the wild type have similar growth profiles, with developmental phases that are reduced in duration compared with *gi2* or *imgi2*: stage I corresponds to the vegetative phase, stage II to flowering, and stage III to senescence. It should be pointed out that the four genotypes in these experiments were grown under conditions of continuous illumination to eliminate circadian clock-mediated effects of *gi2* (Park et al., 1999).

In Figure 2, we were interested in assessing the morphology and pigment contents of fully expanded leaves from the various plants at each developmental stage. Figure 2A shows that the four types of leaves are morphologically similar at stage I but that, by stage II, they have become more diverse in structure. At stage II, *im* and *imgi2* leaves differ from one another and from wild-type and *gi2* leaves; the latter two closely resemble one another. By stage III, *imgi2* leaves have begun to look more like those of *gi2*.

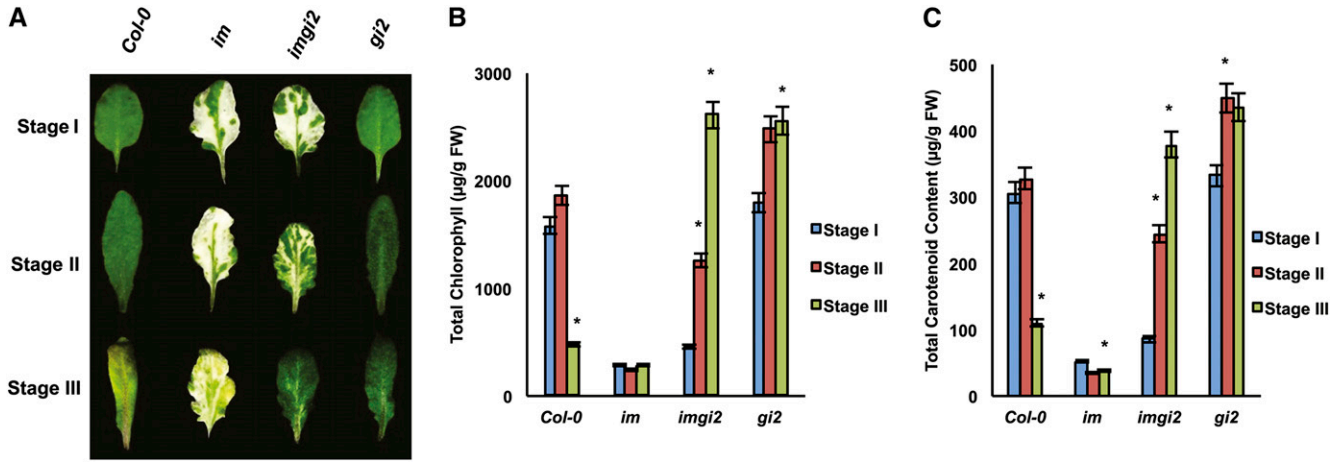

Figure 2. Leaf morphologies and pigment analyses. A, Leaf developmental stages of representative, fully expanded leaves of Col-0, *im*, *imgi2*, and *gi2*. B and C, Chlorophyll and carotenoid contents of the leaves in A. Values represent averages ± SE of three independent replicates relative to stage I plants (*$P < 0.05$). FW, Fresh weight.

Figure 2, B and C, shows the pigment contents (on a fresh weight basis) of the leaves in Figure 2A. Not surprisingly, pigment accumulation in *im* and *imgi2* leaves reflects the extent of their variegation, with *imgi2* closely resembling *im* during early development and *gi2* during late development. However, a striking feature of these analyses is that pigment amounts in *gi2* are significantly higher than in the wild type at all developmental stages. This is also true for stage III (all-green) *imgi2* leaves (i.e. the suppression phenotype is accompanied by high, *gi2*-like pigment levels). Because other *imgi2* traits assessed in Figures 1 and 2 also resemble those found in *gi2* more than in *im*, we conclude that *gi2* is epistatic to *im*, or partially so, with respect to flowering time, leaf morphology, and pigment contents.

Cytokinins Play a Role in *gi*-Mediated Suppression of *im* Variegation

The suppression of variegation that occurs in *imgi2* during stages II and III is striking and is reminiscent of the phenotype of *im* plants that have been detopped; subsequent leaves that emerge are all green (Fig. 3E). Although hormone levels do not necessarily correlate with signal strength, it has been proposed that cytokinins are involved in the detopping response in bean (*Phaseolus vulgaris*; Wang et al., 1977) and tobacco (*Nicotiana tabacum*; Zavaleta-Mancera et al., 1999). These observations prompted us to ask whether cytokinins play a role in the mechanism of variegation suppression in *imgi2*.

As a first approach to address this question, we sprayed 3-week-old Col-0 and *im* for a period of 2 weeks with 6-benzylaminopurine (BAP), a widely used synthetic adenine-type cytokinin. As illustrated in Figure 3, A and C, variegation is suppressed in *im* leaves that emerge after BAP treatment, and this suppression is correlated with sharp, up-regulated expression of genes for type A Arabidopsis response regulators (ARR4–ARR7). These marker genes are rapidly induced at the transcript level in response to cytokinins in Arabidopsis (Hutchison and Kieber, 2002). BAP treatment also causes a delay in the transition to flowering in both Col-0 and *im* (Fig. 3B); as expected, this is accompanied by the down-regulated expression of marker genes for the floral transition, including *CONSTANS*, *FLOWERING LOCUS T*, and *SUPPRESSOR OF CONSTANS1* (Koornneef et al., 1998; Levy and Dean, 1998; Fig. 3C).

In addition to an elevated expression in BAP-treated *im* (Fig. 3C), ARRs are dramatically up-regulated in stage II and III *imgi2* leaves (Fig. 3D). However, this induction is not accompanied by enhanced expression of two representative cytokinin biosynthetic genes, *IPT1* and *IPT5* (Fig. 3D). These genes code for two isozymes of isopentenyltransferase, which catalyzes the first rate-limiting step in the biosynthesis of isoprene cytokinins via the methylerythritol phosphate pathway (Sakakibara, 2006). The lack of response of *IPT1* and *IPT5* might not be surprising, since IPTs are expressed primarily in root tips, immature seeds, young inflorescences, trichomes, and pollen but not in leaves (Miyawaki et al., 2004).

Although we were unable to detect dramatic changes at the transcript level for genes regulating cytokinin biosynthesis in *imgi2* leaves, we considered the possibility of conducting hormone quantification assays to assess the contribution of hormone levels to the cytokinin-mediated events in Figure 3. However, we questioned our ability to identify and obtain enough of the appropriate tissues for analysis. The reason for this is that PTOX is required for chloroplast biogenesis (not for steady-state photosynthesis in the mature leaf; Rosso et al., 2006), and hence it is reasonable to assume that suppression of the *im* defect (by elevated cytokinin signaling) occurs sometime during

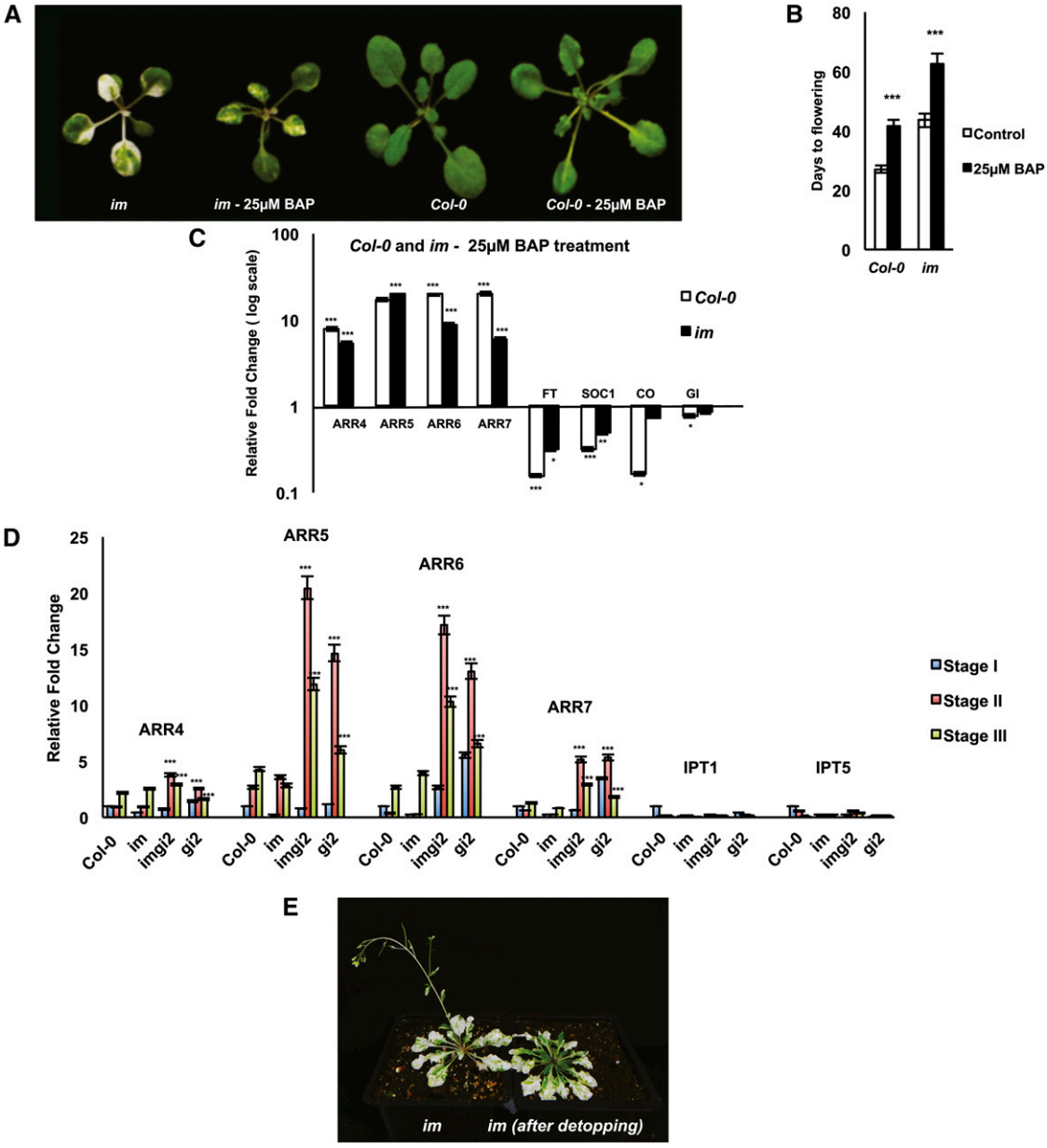

Figure 3. Cytokinin responses. A, Three-week-old *im* and Col-0 plants were sprayed with 25 μM BAP every 3 d for a period of 2 weeks; shown are plants after treatment for 2 weeks. B, Time taken to achieve the floral transition in the plants in A. Values represent averages ± SE of five independent replicates (***$P < 0.001$ relative to control plants). C, Total cell RNAs were isolated from *im* and Col-0 leaves that emerged after the 2-week BAP treatment, and real-time qRT-PCR analyses were performed to examine the expression of cytokinin response genes (*ARR4–ARR7*) and marker genes for the floral transition. Values are normalized to *ACTIN* and relative to control *im* and Col-0 and represent averages ± SE of three technical and two biological replicates (***$P < 0.001$, **$P < 0.01$, *$P < 0.05$). D, Real-time qRT-PCR for cytokinin response genes (*ARR4–ARR7*) and cytokinin biosynthesis genes (*IPT1* and *IPT5*) in Col-0, *im*, *imgi2*, and *gi2* across all three developmental stages. The values are normalized to *ACTIN* and relative to Col-0 stage I plants for each gene and represent averages ± SE of three technical and two biological replicates (***$P < 0.001$ and **$P < 0.01$ relative to Col-0 stage I plants). E, Representative *im* and detopped *im* plants approximately 7 weeks after germination; *im* was detopped at approximately 6 weeks.

the proplastid-to-chloroplast conversion in the leaf meristem and leaf primordium; this occurs sometime just prior to flowering. Knowing these times and being able to identify and collect enough cells that contain developing plastids in the meristem and primordium would be technically challenging. Therefore, we cannot rule out the possibility that hormone levels, as well as the hormone response, are altered in the developing leaf primordium of BAP-treated and *imgi2* leaves.

If *gi*-mediated alterations in cytokinin signaling play a major role in the suppression of *im* variegation, then we might expect to find other traits in *imgi2* that are well-known characteristics of a cytokinin response, such as enhanced leaf blade thickness, starch content, cell number, and rates of chloroplast division (Lichtenthaler and Buschmann, 1978; Stoynova et al., 1996; Werner et al., 2003; Okazaki et al., 2009). In support of this hypothesis, light micrographs of leaf cross sections from the wild type and *imgi2* at the same developmental stage (just prior to flowering, stage I versus stage III, respectively) show that *imgi2* leaves are significantly thicker than normal, devoid of air spaces, and filled with many tightly packed cells, most of which appear to be smaller than normal (Fig. 4A). Figure 4B shows that *imgi2* cells also have higher than normal chloroplast numbers, as illustrated by light microscopy of protoplasts from the wild type and *imgi2* (again, isolated from leaves at the same developmental stages, as in Fig. 4A). The chloroplasts in *imgi2* protoplasts also have significant reductions in surface area, volume, and diameter compared with the wild type (Fig. 4C). These alterations suggest that rates of chloroplast division are enhanced in *imgi2* leaves.

The analyses in Figure 4, B and D, were modeled after experiments in Arabidopsis from the Miyagishima group (Okazaki et al., 2009). They examined the role of cytokinins in chloroplast division in wild-type plants treated with exogenous cytokinins as well as in transgenic plants that overexpress CYTOKININ RESPONSE FACTOR2 (CRF2), a transcription factor induced by cytokinins. They observed that cells in both types of plants had higher chloroplast numbers and smaller chloroplast sizes than wild-type cells (similar to our findings), and they concluded that cytokinin treatment directly enhances chloroplast division. They attributed this enhancement to a specific up-regulation of two cytokinin-responsive genes that encode two essential components of the plastid division apparatus: *PLASTID DIVISION1* (*PDV1*) and *PDV2* (Miyagishima et al., 2006; Glynn et al., 2008). We suggest that a similar cytokinin-dependent mechanism is operative in *imgi2*, inasmuch as the alterations in chloroplast number and size in *imgi2* are accompanied by a sharp up-regulation of *CRF2* and *PDV2* expression (Fig. 4D). Importantly, this up-regulation occurs late in development, coincident with the time when *gi*-mediated effects on cytokinin synthesis/signaling are proposed to be triggered and newly emerging *im* leaves become all green.

In summary, the experiments in Figures 1 to 4 are consistent with the hypothesis that cytokinins play a significant role in *gi2*-mediated suppression of *im* variegation and that the developmental dependence of the suppression phenotype is caused by an up-regulation of cytokinin signaling during stages II and III of plant development. We further propose that this up-regulation results in a reprogramming of plastid and leaf development. These hypotheses raise two important questions. (1) What is the linkage between cytokinin response and *gi*? (2) How does *gi*-mediated cytokinin signaling mechanistically suppress the defect in chloroplast biogenesis caused by the loss of PTOX in *im*?

Mechanistic Relationship between GI and Cytokinin-Mediated Signaling Pathways: A Testable Model

The data in Figures 1 to 4 provide support for the idea that interactions between signaling pathways mediated by GI and cytokinins play an important role in chloroplast biogenesis. To understand how *gi* and cytokinin-mediated signaling are integrated during chloroplast development, we focused on GA signaling as a possible coordinating factor. The reason for this is illustrated in Figure 5, which shows a comprehensive, testable model of how GA signaling might couple GI and cytokinin-mediated signaling pathways. We will then test elements of this model.

The model in Figure 5 is based on the following observations from our experiments and those of others. (1) The transition to flowering in Arabidopsis is controlled in a positive fashion by a number of factors, including photoperiod, light quality, vernalization, and the autonomous pathway, as well as by hormone signaling pathways (Koornneef et al., 1998; Levy and Dean, 1998). (2) Cytokinins delay the transition to flowering in our study (Fig. 3) and in other studies (Wang et al., 1997; McCabe et al., 2001). (3) Cytokinins positively influence chloroplast biogenesis, plastid gene expression, pigment contents, and rates of photosynthesis, although the molecular mechanisms are unclear (Figs. 3 and 4; Parthier, 1979; Lerbs et al., 1984; Chory et al., 1994; Kusnetsov et al., 1994; Yaronskaya et al., 2006, Okazaki et al., 2009). (4) Cytokinin-mediated responses in Arabidopsis are repressed by exogenous application of GA (i.e. up-regulation of GA/GA responses inhibits cytokinin signaling (Greenboim-Wainberg et al., 2005). (5) Arabidopsis *spy* mutants have up-regulated GA responses, and all GA-deficient phenotypes are suppressed in the mutant (Jacobsen and Olszewski, 1993; Jacobsen et al., 1996; Swain et al., 2001). Cytokinin responses are also repressed in *spy* (Greenboim-Wainberg et al., 2005). It has been proposed that SPY represses GA signaling (Tseng et al., 2004) and promotes cytokinin responses either via GA or independently (Greenboim-Wainberg et al., 2005). (6) *spy* mutants suppress the late-flowering phenotype of *gi* (Tseng et al., 2004), indicating that SPY and GI act in concert to regulate the flowering time response in Arabidopsis. Consistent with this idea, SPY and GI interact with one another in yeast two-hybrid experiments (Tseng et al., 2004). (7) SPY controls the transition to flowering in two ways: by inhibiting GA/GA responses (Tseng et al., 2004) and by promoting cytokinin signaling directly (Greenboim-Wainberg et al., 2005; Fleishon et al., 2011). An important element in our proposed mechanism of variegation suppression relies on the observation that GA/GA responses are highly stimulated just prior to the floral transition (Koornneef et al., 1998; Levy and Dean, 1998; Tseng et al., 2004);

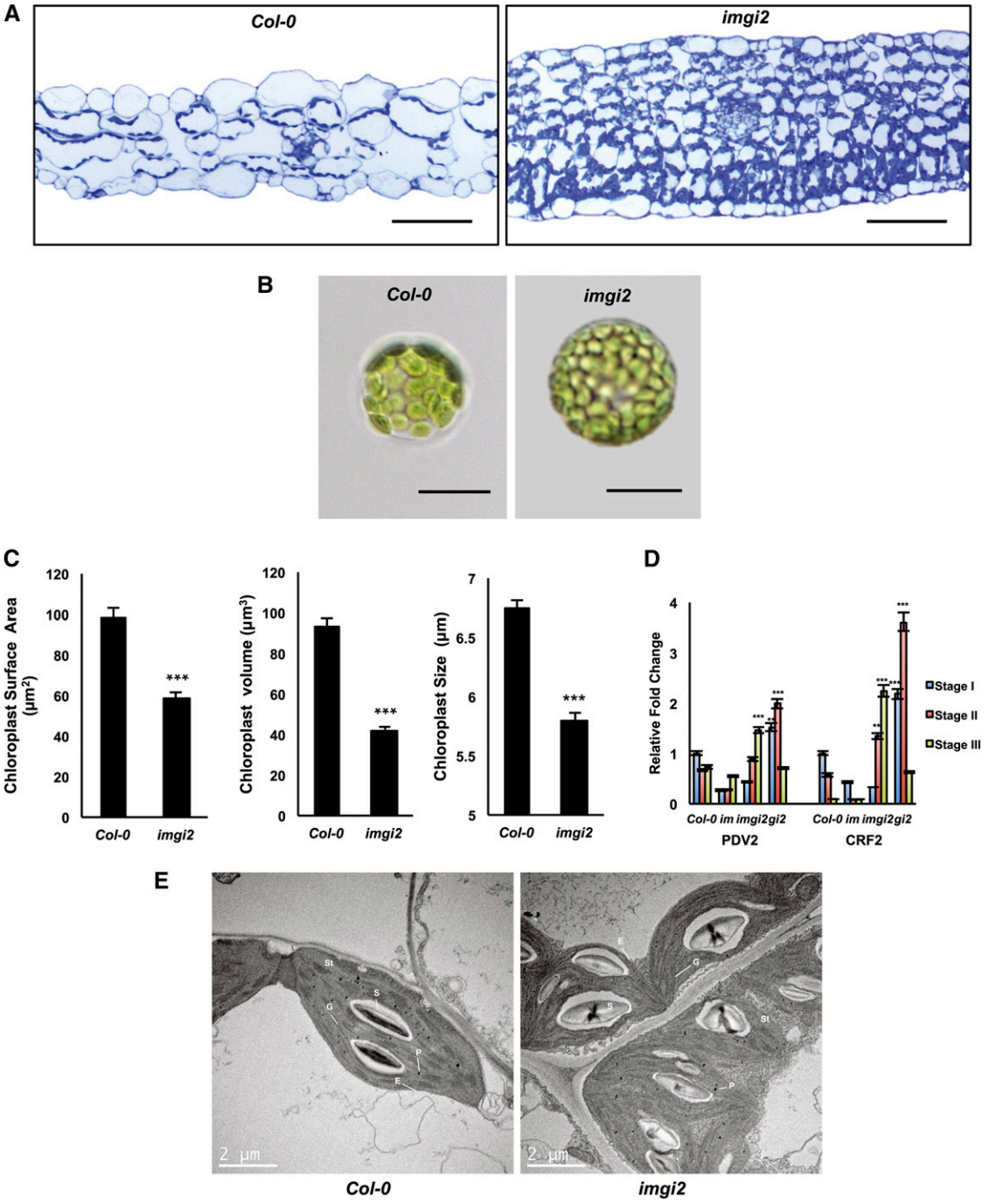

Figure 4. *imgi2* leaf and chloroplast morphologies. A, Light micrographs of cross sections from fully expanded Col-0 and *imgi2* leaves at the same developmental stage (just prior to flowering) stained with 1% (w/v) Toluidine Blue. Bars = 50 μm. B, Bright-field images of *imgi2* and Col-0 protoplasts isolated from leaves (as in A). Bars = 20 μm. C, Chloroplast surface area, volume, and length in Col-0 and *imgi2*. Values represent averages ± SE of 50 independent replicates. *imgi2* plastids show a significant decrease in all three parameters in comparison with Col-0 (***$P < 0.001$). D, Expression analysis using real-time qRT-PCR for *PDV2* and *CRF2* in Col-0, *im*, *imgi2*, and *gi2* across all three developmental stages. Values are normalized to *ACTIN* and relative to Col-0 stage I plants and represent averages ± SE of three technical and two biological replicates (***$P < 0.001$ and **$P < 0.01$). E, Transmission electron micrographs of Col-0 and *imgi2* chloroplasts from leaves just prior to flowering. E, Envelope; G, grana; P, plastoglobule; S, starch granule; St, stroma.

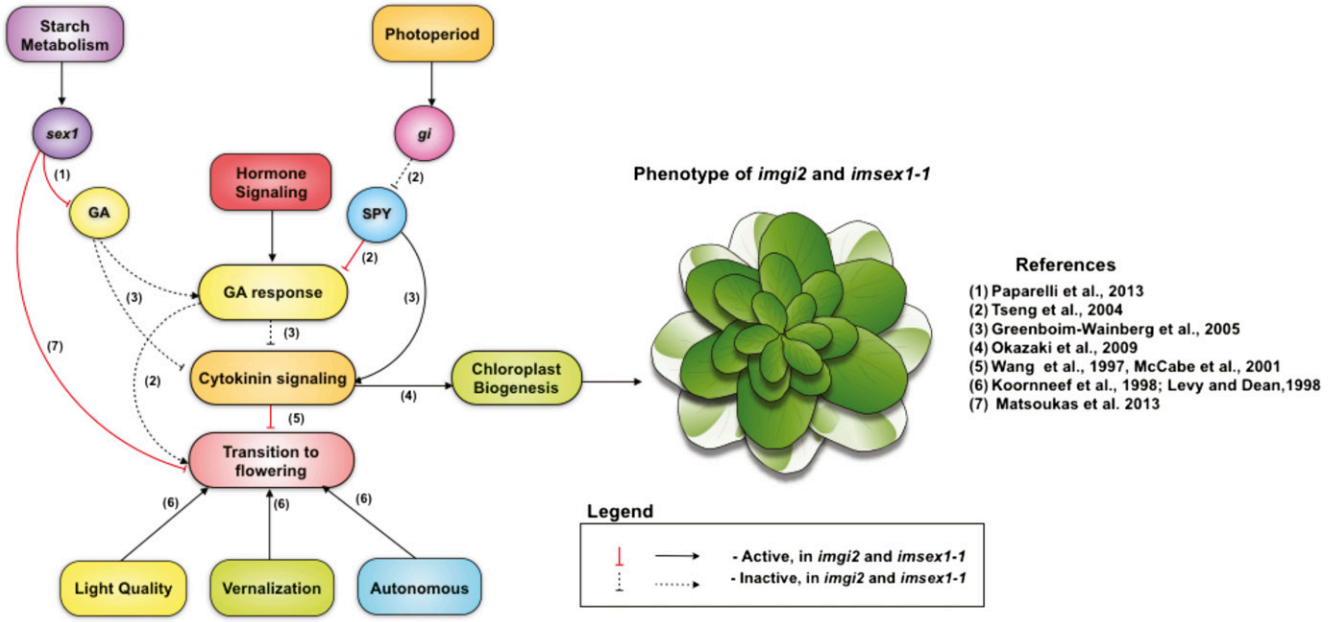

Figure 5. Mechanism of variegation suppression in *imgi2* and *imsex1-1*. Through its interaction with SPY and GA signaling, *gi* causes a derepression of cytokinin signaling that alters chloroplast biogenesis as well as the floral transition time in *imgi2*. *imsex1-1* plants resemble the phenotype of *imgi2* plants, possibly by utilizing the same downstream components (cytokinin-GA signaling pathways) as *imgi2*, causing the suppression of variegation late in development.

that is, a reduced GA response at this time would delay flowering.

Given these considerations, we predict that an absence of GI should result in a derepression of SPY, and this in turn should trigger an inhibition of GA signaling (Fig. 5). Because elevated GA signaling is critical for the transition to flowering, a repression of GA signaling at this time would have two major consequences, both of which we have observed in *imgi2* and both of which are hallmarks of the suppression phenotype: (1) rescue of the variegation phenotype caused by derepression of cytokinin signaling during stage II; and (2) delayed flowering.

This model lends itself to a number of predictions. First, *spy* mutants should be able to reverse the effects of derepressed cytokinin signaling in stage II *imgi2* plants (i.e. the variegation suppression/late-flowering phenotypes of *imgi2* should be abrogated in triple mutants [*imgi2spy*]). To test this hypothesis, we crossed *imgi2* with *spy4* (a strong allele of *spy*; Jacobsen et al., 1996) and identified triple mutants in the segregating F2 population. Consistent with our model, *imgi2spy4* mutants were variegated throughout their development (Fig. 6A), and they flowered after about 6 weeks, similar to wild-type and *im* plants (Fig. 6B). Also as predicted by the model, the alterations in the triple mutant were accompanied by a marked increase in the expression of *GASA4*, a representative GA response gene, and by a decrease in the expression of the cytokinin response genes *ARR4* to *ARR7* (i.e. GA signaling was up-regulated and cytokinin signaling was down-regulated). Taken together, these data indicate that SPY activity is essential to integrate *GI* and chloroplast biogenesis.

A second prediction of our model is that an enhanced GA response should cause a repression of cytokinin signaling and, consequently, a reversal of the suppression phenotypes associated with *imgi2* (all green, delayed flowering). To test this, we sprayed 4-week-old *imgi2* plants with GA_3 for 6 weeks. In accord with our model, the treated plants were variegated at all developmental stages and transitioned to flowering earlier than the nontreated *imgi2* plants (Fig. 6, D and E). In addition, as predicted, these changes were accompanied by a marked down-regulation of the cytokinin response genes *ARR4* to *ARR7* and by an up-regulation of the GA response gene *GASA4* (Fig. 6F). It might be noted that the application of GA_3 to *imgi2* was not as effective as *spy* (in the *imgi2spy4* plants) in promoting time to flowering (Fig. 6, B versus E).

A third prediction of the model in Figure 5 is that the suite of phenotypes associated with *imgi2* should be mimicked by inhibiting GA biosynthesis in *im* (i.e. inhibition of GA signaling [by inhibiting GA biosynthesis] should result in the derepression of cytokinin signaling). To test this hypothesis, we grew Col-0, *im*, *imgi2*, *gi2*, *imgi2spy4*, and *spy4* seeds on Murashige and Skoog (MS) plates supplemented with paclobutrazol (PAC), an inhibitor of GA biosynthesis. Because GA is essential for germination, we anticipated that only seeds in the *spy4* background should germinate; this was confirmed (Fig. 6G). To inhibit GA in a mutant lacking PTOX without inhibiting germination, we grew *im* on soil for 2 weeks and then watered the plants with

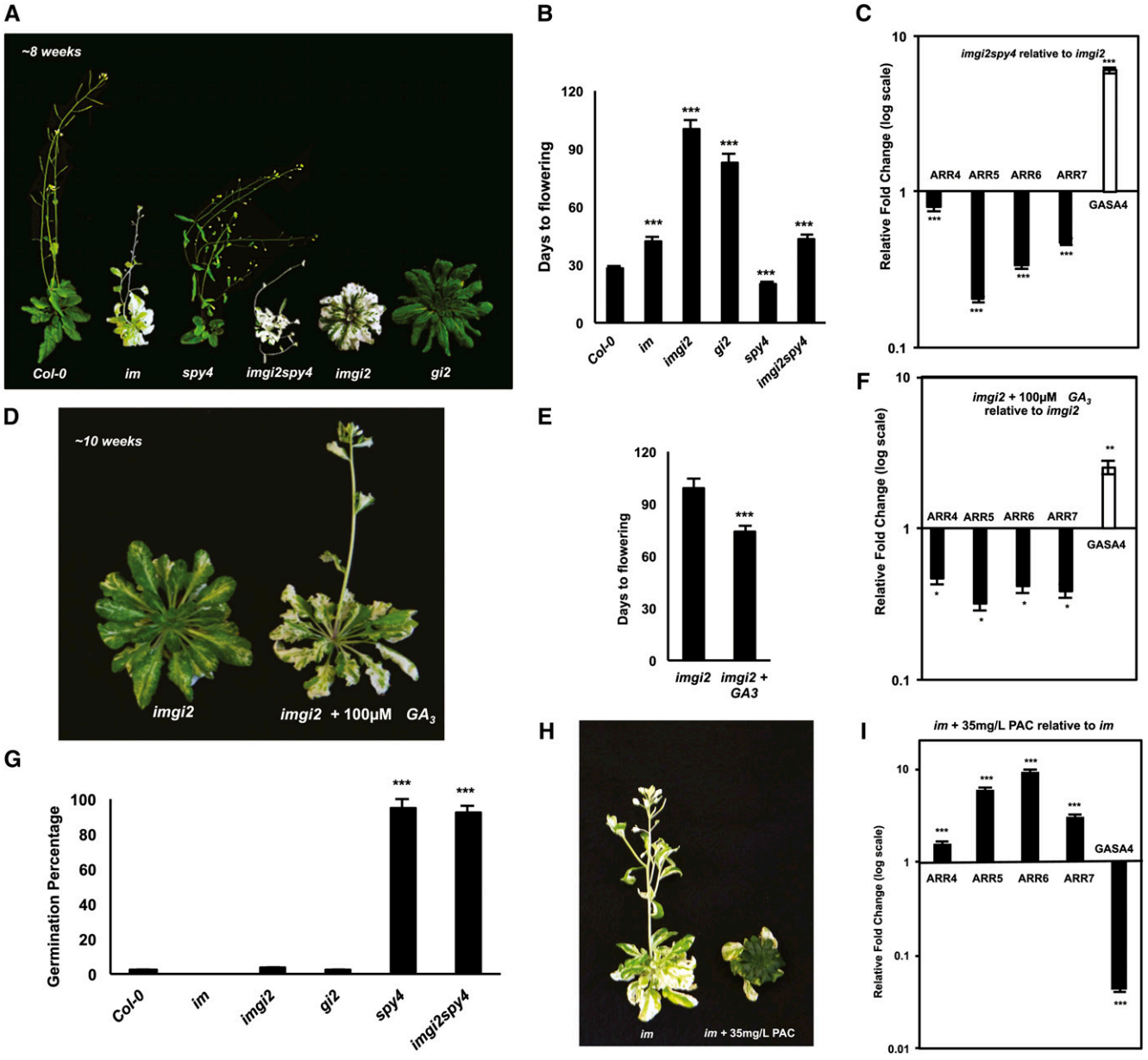

Figure 6. Rescue of *imgi2* by *spy* and GA. A, Representative Col-0, *im*, *spy4*, *imgi2spy4*, *imgi2*, and *gi2* at approximately 8 weeks after germination. Plants were grown as in Figure 1A. B, Time taken to achieve the floral transition in Col-0, *im*, *spy4*, *imgi2spy4*, *imgi2*, and *gi2*. Values represent averages ± SE of five independent replicates (***$P < 0.001$ relative to Col-0 plants). C, qRT-PCR analysis of cytokinin response genes (*ARR4–ARR7*) and a GA response gene, *GASA4*, in *imgi2spy4* and *imgi2* at the same developmental stage (just prior to flowering). Expression values were normalized to *ACTIN* and relative to *imgi2* plants and represent averages ± SE of three technical and two biological replicates (***$P < 0.001$). D, Four-week-old *imgi2* plants were watered with or without 100 μM GA_3 twice weekly for 6 weeks. E, Time taken to achieve the floral transition in the plants in D. Values represent averages ± SE of five independent replicates (***$P < 0.001$ relative to *imgi2* plants of the same age). F, qRT-PCR analysis of cytokinin response genes (*ARR4–ARR7*) and a GA response gene, *GASA4*, in the plants in D. Values were normalized to *ACTIN* and relative to nontreated *imgi2* plants and represent averages ± SE of three technical and two biological replicates (**$P < 0.01$ and *$P < 0.05$). G, Col-0, *im*, *imgi2*, *gi2*, *spy4*, and *imgi2spy4* seeds were plated on MS medium supplemented with 35 mg L^{-1} PAC. The average germination percentage was determined after 10 d from 75 seeds sown on three independent plates (25 seeds per plate). Values represent averages ± SE for percentage of seedlings that germinated on each of the plates (***$P < 0.001$ relative to Col-0). H, Representative *im* and PAC-treated *im* plants. Plants were grown as in Figure 1A and watered with or without PAC (35 mg L^{-1}); PAC treatment commenced approximately 2 weeks after germination and continued for another 4 weeks. I, qRT-PCR analysis of cytokinin response genes (*ARR4–ARR7*) and the GA response gene, *GASA4*, in the plants in H (i.e. 6 weeks after germination). Expression values were normalized to *ACTIN* and relative to *im* control plants and represent averages ± SE of three technical and two biological replicates (***$P < 0.001$).

PAC (35 mg L^{-1}) for 4 weeks. Consistent with our hypothesis, PAC treatment suppressed the *im* variegation phenotype and newly emerging leaves were all green (Fig. 6H). As anticipated if PAC inhibits GA, this suppression was accompanied by a sharp decrease in the expression of the GA response gene *GASA4* (Fig. 6I) as well as by a marked increase in expression of the cytokinin response genes *ARR4* to *ARR7*. These findings are in accord with the model and indicate that an inhibition of GA results in a derepression of cytokinin signaling.

In summary, we conclude that there is a strong correlation between the greening/late-flowering phenotypes associated with *imgi2* and the cytokinin response. We also conclude that GA signaling and SPY are essential components that integrate *gi* and cytokinin signaling to control chloroplast biogenesis.

How Does Cytokinin-Mediated gi Signaling Mechanistically Suppress im Variegation?

Although it is widely recognized that cytokinins modulate processes of chloroplast biogenesis, the mechanisms are poorly understood (Parthier, 1979; Lerbs et al., 1984; Chory et al., 1994; Kusnetsov et al., 1994; Yaronskaya et al., 2006). According to the threshold hypothesis of *im* variegation, developing plastids with lower than threshold EPs (i.e. relatively oxidized PQ pools) differentiate into normal chloroplasts and give rise to green sectors in the mature leaf, whereas developing plastids with higher than threshold EPs (i.e. overreduced PQ pools) accumulate phytoene and become blocked in the production of photoprotective, downstream carotenoids; these plastids are susceptible to photooxidation and give rise to white sectors in mature leaves (Rosso et al., 2009). To identify the mechanism(s) by which *gi2* suppresses *im* variegation, we reasoned that the signaling pathways in Figure 5 likely result in the production of factors that cause a relaxation of EPs, such that more developing plastids have EPs within the range compatible with normal chloroplast biogenesis. Thus, our question became: how do cytokinins and GA control EPs?

To address this question, we felt that it would be helpful to first obtain baseline information about the ultrastructure and protein composition of *imgi2* chloroplasts. Figure 4E shows transmission electron micrographs of representative chloroplasts from fully expanded wild-type and *imgi2* leaves just prior to flowering: *imgi2* chloroplasts are smaller than normal (thus confirming the protoplast data in Fig. 4, B and C) but otherwise have normal-appearing internal membrane structures. We next conducted western immunoblot analyses to examine the accumulation of seven representative photosynthetic proteins from *im*, *gi2*, *imgi2*, and Col-0 leaves at developmental stages I to III; the proteins were loaded on the gels on an equal fresh weight basis. Figure 7 shows that, during stage I, each of the seven proteins accumulates to a similar extent in *gi2* and the wild type and also to a similar, although reduced, extent in *im* and *imgi2*; the decreases in *im* and *imgi2* are expected and caused by the presence of white tissues in the whole-leaf samples (Aluru et al., 2007). During stage II, the pattern of protein accumulation in *imgi2* begins to resemble that of *gi2* (a notable exception being D1), such that by stage III, all seven proteins have accumulated to high levels and the *imgi2* and *gi2* profiles are indistinguishable. Stage III wild-type and *im* leaves, on the other hand, are senescent and, not surprisingly, have much reduced amounts of all seven proteins.

Taken together, the data in Figures 4E and 7 indicate that *gi2* is able to attenuate the impact of a loss of PTOX on chloroplast biogenesis late in plant development, such that all-green leaves are produced whose chloroplasts resemble those in *gi2* with respect to ultrastructure and protein composition. This suggests that *gi2* is epistatic to *im* with respect to these traits, commencing at stage II, thus expanding the list of traits enumerated earlier (i.e. leaf morphology, pigment composition, and flowering time; Figs. 1, A and B, and 2, A–C) and the expression of genes for the cytokinin response (Figs. 3D and 4D). Given the widespread number of *gi* traits that are epistatic to *im*, we asked whether the suppression of EPs in *im* could be caused by one or more *gi* phenotypes that have been documented over the years that could theoretically ameliorate EPs. These include an elevated expression of detoxifying enzymes such as SOD and APX in the presence of paraquat (Cao et al., 2006) and enhanced accumulation of starch (Eimert et al., 1995). Do either of these factors play a role in *gi*-mediated suppression of *im* variegation?

ROS Detoxification. One of the most intriguing phenotypes of *gi* is its resistance to hydrogen peroxide (H_2O_2) and paraquat (Kurepa et al., 1998a). Paraquat is a superoxide (O_2^-) radical-generating herbicide that acts by intercepting the flow of electrons at PSI (Preston, 1994); O_2^- and H_2O_2 are produced by an interaction of paraquat radicals with molecular oxygen (Slade, 1966). The resistance of *gi2* to paraquat is caused by an elevated expression of the chloroplast-detoxifying enzymes SOD and APX in the presence of the herbicide (Cao et al., 2006).

To obtain an overview of the role of ROS generation and quenching in the suppression of *im* variegation, we assayed the accumulation of O_2^- and H_2O_2 in *im*, *gi2*, *imgi2*, and Col-0 leaves by nitroblue tetrazolium (NBT) and 3,3′-diaminobenzidine (DAB) staining, respectively. Figure 8A shows that ROS accumulation is very low in *gi2* throughout development, consistent with previous observations (Kurepa et al., 1998a), but that O_2^- and H_2O_2 levels are high in *im* and *imgi2*, especially early in development. Strikingly, *gi2* is able to sharply reduce the high amounts of ROS that are present in *im*. This suppression occurs during stages II and III of *imgi2* development (when newly emerging leaves are becoming all green) and is accompanied by prolonged, high-level expression of stromal and

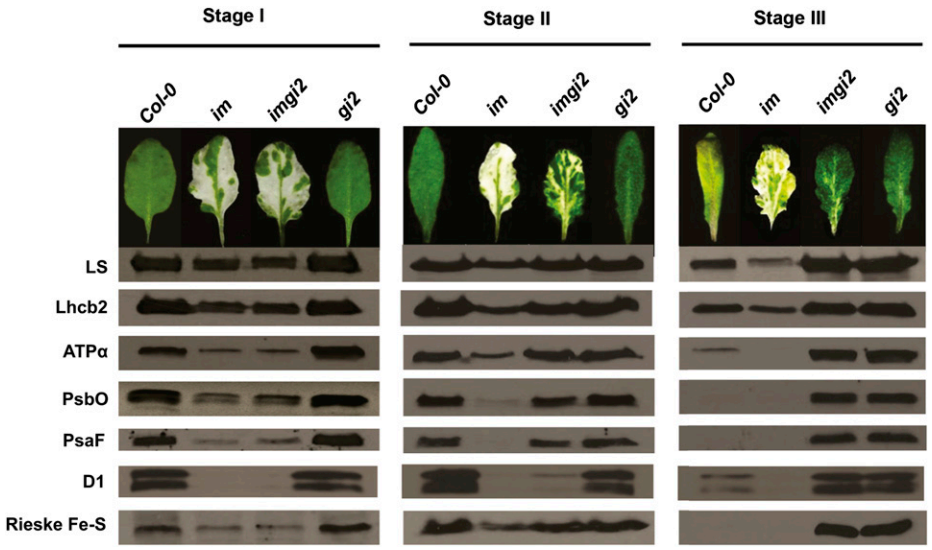

Figure 7. Photosynthetic protein accumulation. Total leaf proteins were isolated from the top two fully expanded rosette leaves of Col-0, *im*, *imgi2*, and *gi2* at stages I to III. The proteins were loaded on an equal fresh weight basis for electrophoresis via 12% SDS-PAGE. Immunoblot analysis used polyclonal antibodies to the large subunit of Rubisco (LS), the light-harvesting complex protein (Lhcb2), the α-subunit of ATP synthase (ATPα), PSII subunit O (PsbO), PSI subunit F (PsaF), PSII reaction center protein (D1), and the Rieske Fe-S center of the cytochrome b_6f complex (Rieske Fe-S).

thylakoid APXs (Shigeoka et al., 2002; Fig. 8B). Similar to *imgi2*, *gi2* has high levels of APX expression at all three developmental stages; in contrast, expression levels fall markedly in the wild type and *im* after stage I (just prior to flowering) and either continue to fall (thylakoid APX) or increase dramatically (stromal APX) during senescence (stage III). Considered together, the data in Figure 8 suggest that *gi2* is epistatic to *im* with respect to having an enhanced ROS scavenging capacity during late plant development. We conclude that this could be a contributing factor to reduce EPs in *imgi2*, thus suppressing variegation.

Starch Accumulation. Another well-characterized phenotype of *gi* that has the potential to ameliorate EPs is starch accumulation (Eimert et al., 1995). To explore this question in *imgi2*, we monitored leaf starch content by staining intact plants (the wild type, *im*, *imgi2*, and *gi2*) with Lugol's iodine solution; the plants were removed from the soil and stained when they were at the same developmental stage (just prior to flowering). Figure 9A shows that starch levels are significantly elevated in *imgi2* and *gi2* compared with *im* and the wild type. This conclusion was confirmed by quantitative measurements: vegetative leaves of prebolting *imgi2* and *gi2* accumulate about twice as much starch as

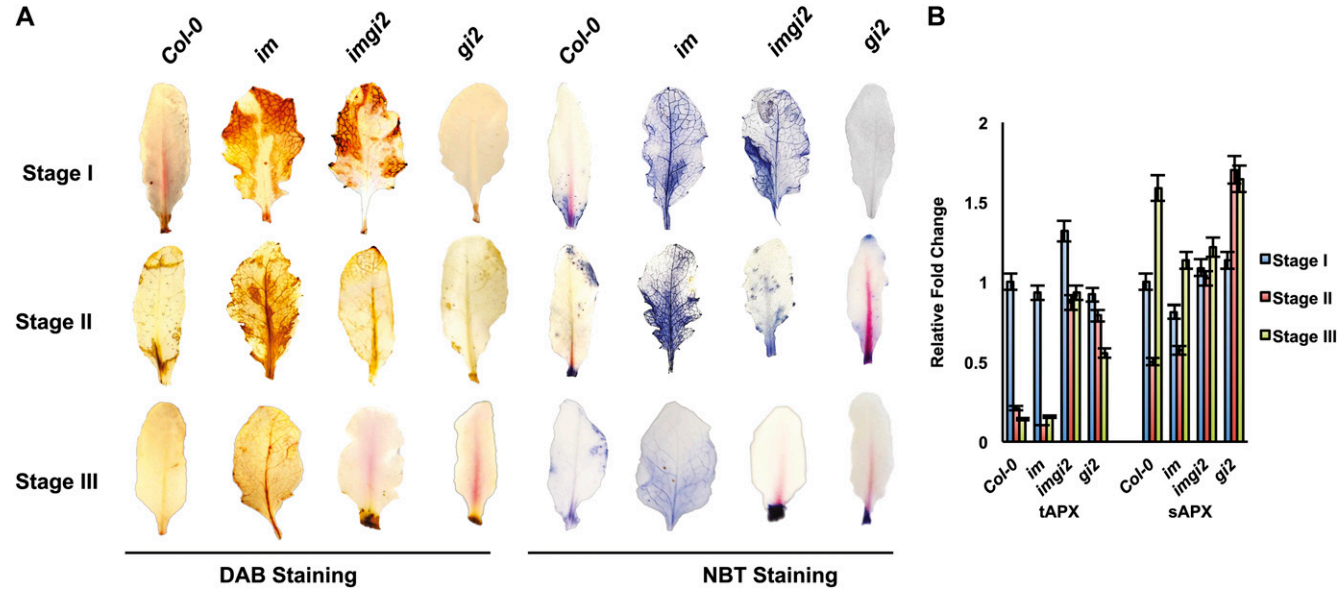

Figure 8. ROS accumulation. A, DAB and NBT staining to detect H_2O_2 and O_2^-, respectively, in Col-0, *im*, *imgi2*, and *gi2* across all three developmental stages. B, Expression analysis using real-time qRT-PCR for stromal APX (sAPX) and thylakoid APX (tAPX) genes in Col-0, *im*, *imgi2*, and *gi2* at stages I to III. Expression values are normalized to *ACTIN* and relative to stage I Col-0 plants and represent averages ± SE of three technical and two biological replicates.

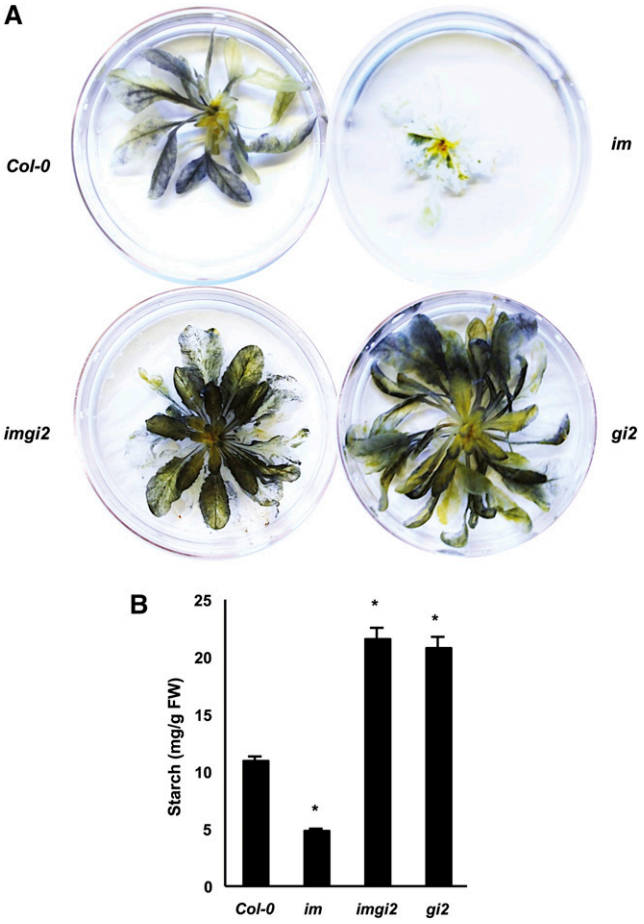

Figure 9. Starch accumulation. A, Qualitative analysis of starch accumulation in Col-0, *im*, *imgi2*, and *gi2* at the same developmental stage (just prior to flowering). Plants were removed from the soil and stained with potassium iodide/iodine solution (Lugol's iodine), destained in water for 1 h, and then photographed. B, Quantitative analysis of starch levels in Col-0, *im*, *imgi2*, and *gi2* at the same developmental stage (prior to flowering). Values represent averages ± SE of three independent replicates (*$P < 0.05$ relative to Col-0 plants). FW, Fresh weight.

the wild type on a fresh weight basis (Fig. 9B). The high levels of starch are also apparent from electron micrographs (Fig. 4).

One explanation for these results is that *imgi2* and *gi2* have higher than normal rates of carbon assimilation. To test this hypothesis, we generated carbon assimilation rate-internal CO_2 concentration curves at a constant photosynthetic photon flux density (200 μmol m^{-2} s^{-1}) using fully expanded leaves from plants at the same stage of development (just prior to flowering). Figure 10C shows that carbon assimilation rates are significantly higher in the all-green leaves of *imgi2* and *gi2* versus the wild type; lower than normal values for *im* reflect the presence of contaminating white sectors in the leaf samples (Aluru et al., 2007). It is likely that the enhancement in assimilation in *imgi2* is caused, in part, by increased photosynthetic electron transport capacity, inasmuch as chlorophyll fluorescence analyses revealed that *imgi2* leaves have lower than normal EPs and higher than normal electron transport rates (Fig. 10, A and B). The latter experiments were conducted under a range of light intensities using leaves from *imgi2* and the wild type at the same stage of development (just prior to flowering).

Regardless of the precise mechanism, the data in Figures 9 and 10 indicate that *gi2* is epistatic to *im* with respect to carbon assimilation and starch accumulation. Enhanced rates of carbon assimilation and photosynthetic electron transport in *imgi2* would be a powerful way to decrease EP thresholds and promote chloroplast biogenesis.

Can starch excess1 Rescue im? Given that enhanced ROS scavenging and carbon assimilation are two mechanisms that could play a direct role in *gi*-mediated relaxation of EPs in *im*, we wanted to examine whether either of these is sufficient to suppress *im* variegation. Early attempts to rescue the *im* variegation phenotype by the overexpression of components of the ROS scavenging system (SOD and APX) were not successful, likely because these components are redundant and act in concert to scavenge ROS (Giacomelli et al., 2007). To examine whether starch accumulation is sufficient, we crossed *im* with *starch excess1* (*sex1*), a well-characterized starch accumulation mutant that, interestingly, also displays a late-flowering phenotype (Matsoukas et al., 2013); we used null alleles of both *im* (*spotty* allele) and *sex1* (*sex1-1*; Yu et al., 2001) for this cross. SEX1 is a starch-related α-glucan/water dikinase that controls the accessibility of degradative enzymes to the starch granule, and starch accumulates in *sex1* mutants because it lacks this accessibility (Yu et al., 2001; Yano et al., 2005). Surprisingly, we found that *imsex1-1* double mutants recapitulate the phenotype of *imgi2* (i.e. they are late flowering [approximately 10 weeks to achieve the floral transition] and produce variegated leaves early in development but all-green leaves later in development; Fig. 11). *imsex1-1* and *sex1-1* plants also have enhanced rates of carbon assimilation compared with the wild type, similar to that observed for *gi2* and *imgi2* (Fig. 10C). Considered together, these data indicate, first, that *sex1*-mediated signaling is able to rescue *im* variegation in a development-specific manner, and second, that *sex1* is epistatic to *im* with respect to flowering time, photosynthetic carbon assimilation, and chloroplast biogenesis, commencing late in plant development. This suggests that *imsex1-1* and *imgi2* resemble one another with respect to a number of traits.

DISCUSSION

Signaling Events That Control Chloroplast Biogenesis

For a number of years, we have used *im* as a tool to gain insight into mechanisms of photosynthetic electron transport and chloroplast development (Yu et al.,

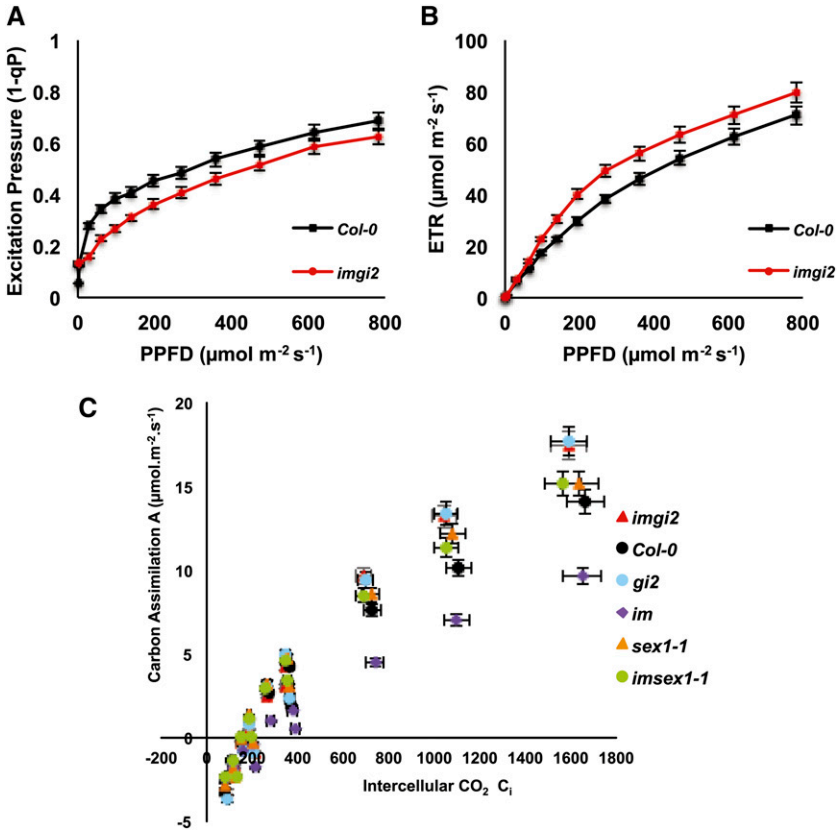

Figure 10. Photosynthesis and carbon assimilation. A and B, Chlorophyll fluorescence parameters were measured on detached leaves from *imgi2* and Col-0 under varying light intensities. Excitation pressure is a measure of the redox state of the first stable electron acceptor of PSII and is quantified using the parameter 1-qP (photochemical quenching), and ETR is the relative linear electron transport rate. C, CO_2 assimilation rates (A) with respect to the internal CO_2 concentrations (C_i) in Col-0, *im*, *imgi2*, *gi2*, *imsex1-1*, and *sex1-1* plants at the same developmental stage (just prior to flowering). The A-C_i curves were plotted at a photosynthetic photon flux density of 200 μmol m^{-2} s^{-1}. Values represent averages ± SE of five biological replicates.

2007; Liu et al., 2010; Foudree et al., 2012; Putarjunan et al., 2013). These studies have included the characterization of second-site suppressors that rescue the variegation phenotype of *im*, producing all-green plants. These suppressors have allowed us to identify elements that are important for PTOX activity and, more broadly, elements that integrate pathways of chloroplast biogenesis (Fu et al., 2012; Putarjunan et al., 2013). Because PTOX plays a crucial role in maintaining the redox state of developing thylakoids, a unique feature of *im* bypass suppressors is that they provide a way to access factors that play a role in the early events of chloroplast biogenesis but that are difficult to identify using techniques of biochemistry and molecular biology because of their abundance and/or location in difficult-to-study meristematic and leaf primordial tissues. In this report, we found that the defect in *im* plastids can be suppressed by *gi* in developing chloroplasts of leaves that emerge late in plant development. Interestingly, Rédei (1962, 1963) crossed *im* with *gi* over 50 years ago as way to generate vigorous *im* plants for study but did not report on the late-greening phenotype of the double mutant; he also assumed that *gi* merely provided a growth phenotype and did not affect the *im* plastid phenotype per se.

Importantly, our analyses enabled us to develop a testable model of *gi*-mediated pathways that control chloroplast biogenesis using *im* as a reporter (Fig. 5). This model is based on published observations as well as on findings in this study. The robustness of the model is reflected in our ability to confirm elements of it experimentally. One of our central findings is that *gi* mediates chloroplast biogenesis (and flowering time) via an effect on GA and cytokinin signaling. Support

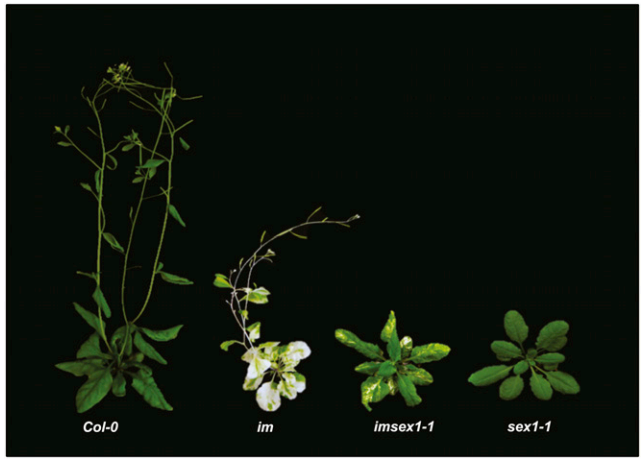

Figure 11. Suppression of variegation in *imsex1-1* double mutants. Representative Col-0, *im*, *imsex1-1*, and *sex1-1* plants are shown approximately 10 weeks after germination. The *imsex1-1* plants are late flowering and produce variegated leaves early in development but all-green leaves later in development, similar to *imgi2* plants.

for this hypothesis came from our observation that *spy* reverses the variegation suppression and late-flowering phenotypes of *imgi2*. This indicates that SPY activity plays an important role in chloroplast biogenesis and also highlights the significance of cross talk between the GA and cytokinin signaling pathways in the plastid development process. While our data suggest that the hormone response plays a dominant role in the suppression mechanism, we cannot rule out the possibility that hormone levels are also altered. Determining whether this is the case would be a challenging undertaking because it would require the ability to identify and obtain enough tissues in which the chloroplasts of the meristem and leaf primordium are still developing (i.e. the stage at which PTOX first functions and when the *im* defect is suppressed).

In this context, it is worth emphasizing that the uniqueness of *imgi2* lies in its ability to manipulate hormone signaling pathways that are essential for the floral transition in such a manner that developmental reprogramming of *imgi2* plastids occurs at this time. In other words, the defect in *im* plastids is suppressed late rather than early in development and is not expressed continuously throughout development, as might be expected with constitutive overexpression of cytokinin biosynthesis/response genes. Our model emphasizes GA, because GA is involved in stimulating the transition to flowering by transcriptionally activating genes directly controlling the floral transition; GA/GA responses also are expressed most highly just prior to this stage (Koornneef et al., 1998; Levy and Dean, 1998. Furthermore, transcriptomic analyses in *gi* mutants of rice (*osgi-1*) have revealed remarkable increases in the transcript accumulation of genes coding for GA 2-oxidase, which is involved in inactivating bioactive GAs (Itoh and Izawa, 2011).

The phenotypic similarity between *imgi2* and *imsex1-1* is striking and raises questions about the integration of *sex1* into the model in Figure 5. Although speculative at this point, one possibility is that there is a convergence of *gi*- and *sex1*-mediated pathways at GA/GA signaling and the utilization of identical elements downstream from GA that involve derepression of cytokinin signaling. Support for this hypothesis comes from recent studies showing that GA biosynthesis is repressed in *sex1-1* as a response to sugar starvation, which arises from the primary lesion in the mutant and its inability to break down starch (Paparelli et al., 2013). Interestingly, *gi* mutants display a similar sugar starvation phenotype (Cao et al., 2007). A detailed understanding of interactions between *sex1* and GA awaits further investigation.

It should be noted that exogenously supplied cytokinins are able to rescue the phenotypes of other nuclear gene-induced variegations like *pale cress* (*pac*; Grevelding et al., 1996) and *amidotransferase-deficient2* (*atd2*; van der Graaff et al., 2004), producing all-green plants. Although the function of the PAC gene is unknown, *pac* mutants have a light-conditional phenotype that results in photooxidized plastids early in development, perhaps because PAC affects the accumulation of carotenoids and abscisic acid (Grevelding et al., 1996; Meurer et al., 1998; Holding et al., 2000). On the other hand, *atd2* (and other alleles of the same mutant gene, such as *altered APX2 expression13* and *chloroplast import apparatus1*) defines the gene for ATASE2, the first enzyme of purine biosynthesis, and loss of this critical enzyme has pleiotropic effects, including a light-conditional phenotype and the accumulation of ROS (Sun et al., 2001; van der Graaff et al., 2004; Woo et al., 2011). Because *pac* and *atd2* have different primary lesions in chloroplast development, we consider it likely that their rescued phenotypes, following cytokinin treatment, rely on the utilization of different batteries of cytokinin-regulated genes and perhaps different processes than those utilized in *imgi2*. In this context, it will be interesting to determine whether cytokinin-treated *pac* and *atd2* are also late flowering, similar to BAP-treated *im*, and whether the *pac* and *atd2* variegations can be suppressed by *gi* and *sex1-1*.

Molecular Mechanism(s) of *im* Suppression

Based on our current conception that EP thresholds govern *im* variegation (Rosso et al., 2009), the findings in this article support the idea that a lack of GI attenuates EP thresholds in *imgi2* via an aberrant derepression of cytokinin signaling during late plant development. This causes suppression of the *im* defect, because EP thresholds are reduced to such an extent that all (or nearly all) developing plastids in the leaf primordium are able to differentiate into photosynthetically competent chloroplasts. Given that cytokinins play a pivotal role in photosynthesis and chloroplast biogenesis, it is perhaps surprising that the molecular mechanisms are so poorly understood. In perhaps the best-studied case, cytokinin control of chloroplast division has been traced to specific upregulation of two nuclear genes whose products, PDV1 and PDV2, are imported into the plastid posttranslationally, where they serve as components of the plastid division machinery (Miyagishima et al., 2006; Glynn et al., 2008). By analogy, our question can be stated as: how does cytokinin signaling compensate for a loss of PTOX at the level of the photosynthetic membrane; that is, what are the changes in cytokinin-mediated gene expression that mitigate EPs during chloroplast biogenesis?

One widely used approach to address this type of question involves the identification of candidate genes via global expression analyses, followed by rescue of a mutant phenotype. This approach is fraught with difficulties (e.g. too many genes, and gene interactions, to sort through) and subject to a great degree of serendipity. We were able to avoid these problems by taking advantage of the epistatic interactions between *gi2* and *im*, which allowed us to narrow down the possible factors that ameliorate EPs in *imgi2* by asking whether any of the *gi2* phenotypes characterized over the past

50 years of GI research could logically play a role in modulating EPs and, thereby, rescue the *im* defect.

The first *gi* phenotype we examined was ROS scavenging capacity, which is up-regulated in *gi* in the presence of paraquat, a ROS generator (Cao et al., 2006). Given that developing *im* membranes are over-reduced, *im* also acts as a ROS generator (Ivanov et al., 2012); this was confirmed in Figure 8. We found that ROS accumulation is drastically reduced in *imgi2* in late plant development to levels that are characteristic of *gi2* (i.e. *gi2* is epistatic to *im* with respect to this trait). This leads to the reasonable hypothesis that derepression of cytokinin signaling in late *imgi2* development causes an up-regulation of gene expression for ROS detoxification enzymes, as illustrated for APX (Fig. 8B), and that this results in an enhanced ROS scavenging capacity in developing *imgi2* plastids, a reduction of EPs, and suppression of the *im* defect. This proposal is consistent with the observations of others that cytokinin signaling and chloroplast ROS scavenging capacity are linked (Pogany et al., 2004; Cortleven et al., 2014) and also with the finding that plastid-localized ROS scavenging enzymes like SOD and APX are specifically increased in maize (*Zea mays*) seedlings treated with PAC (Pinhero et al., 1997). In accord with our model, the latter might be a cytokinin response, rather than a GA response, inasmuch as inhibition of GA (via PAC) would be anticipated to derepresses cytokinin signaling.

The second feature of *gi2* that we investigated was its striking ability to accumulate starch. We discovered that this is accompanied by enhanced rates of photosynthetic carbon assimilation. Using biochemical and molecular techniques, we have previously shown that the green sectors of fully expanded *im* leaves behave as sources and the whites sectors as sinks. The green sectors also have enhanced photosynthetic capacity, as monitored by chlorophyll fluorescence, oxygen evolution, and carbon fixation rates (Aluru et al., 2001, 2007). Profiling experiments have revealed that this enhancement is likely caused by a reprogramming of photosynthetic gene expression in the green cells, perhaps elicited during leaf development in response to sink demand (i.e. elevated photosynthetic capacity is part of a growth strategy to compensate for total reductions in source tissue; Aluru et al., 2001, 2007). This explanation does not seem to apply to *imgi2*, however, because *imgi2* plants are not variegated. Rather, we propose that *gi2* is epistatic to *im* with respect to this trait and that when it is combined with *im* in the double mutant, one consequence is that EPs are attenuated to such an extent that the *im* defect is suppressed. Because we cannot rule out the possibility of interactions between *im* and *gi2* that might modify the elevated photosynthesis trait, *gi2* (versus *imgi2*) might be a cleaner system to assess mechanistically how photosynthetic rates are controlled by cytokinin. The answer to this question has obvious implications for practical and applied studies of mechanisms of carbon sequestration.

In this context, it should be pointed out that *imsex1-1* suppressors resemble the phenotype of *imgi2*, perhaps because both SEX1 and GI utilize the same pathways downstream from GA (as discussed earlier). If this is the case, several predictions can be made. For example, *sex1-1* should show the same suite of chloroplast phenotypes as *gi2*, including enhanced ROS scavenging capacity in response to paraquat. Predictions such as these can be tested in future investigations. Other mutants with a starch accumulation/late-flowering phenotype also might be found that rescue *im*, and if these mutants utilize the pathways in Figure 5, they could be used to investigate elements and interactions upstream of GA (like GI and SEX1) that regulate chloroplast biogenesis.

Given what we know about the primacy of redundancy and plasticity in signaling pathways in plants, it is perhaps naïve to expect that a single mechanism would be responsible for suppressing *im* variegation, especially in a genetic background that involves loss of a factor as critical for the cell as GI. As illustrated here, this loss leads to alterations in hormone signaling that could conceivably impact a number of processes that affect EPs. Two prime candidates identified in this article include enhanced photosynthesis and enhanced ROS scavenging, and we propose that these two constitute a prominent response pathway in chloroplasts. We conclude that our experiments show the utility and power of the suppressor approach for gaining insight into pathways and processes that govern chloroplast biogenesis.

MATERIALS AND METHODS

Plant Material and Growth Conditions

All Arabidopsis (*Arabidopsis thaliana*) plants in this study were grown on soil at 22°C under continuous illumination (approximately 100 μmol m^{-2} s^{-1}). Because *im* is light sensitive, it was germinated for 10 d under low illumination (15 μmol m^{-2} s^{-1}) prior to transfer to normal light conditions. Mutant crosses in the *im* background were treated in a similar manner. *gi2* and *sex1-1* seeds were obtained from the Arabidopsis Biological Resource Center, and *spy4* seeds were a generous gift from Neil Olszewski (University of Minnesota, St. Paul). Genotypes of double and triple mutant progeny were identified by PCR using the derived cleaved-amplified polymorphic sequence primers in Supplemental Table S1.

Pigment Analyses

The two top pairs of fully expanded rosette leaves from Col-0, *im*, *imgi2*, and *gi2* at stages I to III of development were harvested and ground in liquid N_2. Pigments were extracted in the dark at 4°C using 19:1 ethanol:H_2O (v/v). Total chlorophyll and carotenoid contents were calculated as described (Lichtenthaler, 1987).

Hormone Response Assays

Three-week-old Col-0 and *im* plants were sprayed with 25 μM BAP (Sigma-Aldrich) once every 3 d for a period of 2 weeks. Leaves that emerged after treatment were used for experimentation. For treatment with GA_3, *imgi2* plants were sprayed with 100 μM GA_3 (dissolved in water) at around 4 weeks after germination for a period of 6 weeks (two times per week). Endogenous GA was inhibited using PAC (Sigma-Aldrich) at a concentration of 35 mg L^{-1}. For plate assays, MS plates were supplemented with 35 mg L^{-1} PAC, and for soil assays, 2-week-old *im* plants were watered with PAC for a period of 4 weeks (three times per week).

Light and Transmission Electron Microscopy

Fully expanded rosette leaves from Col-0 and *imgi2* plants at the same developmental stage (stages I and III, respectively) were used for light and transmission electron micrograph imaging. Samples were fixed, stained, and examined as described by Horner and Wagner (1980).

Chloroplast Ultrastructure

Chloroplast surface area, volume, and size were calculated from light micrograph images of protoplasts from Col-0 and *imgi2* as described previously (Li et al., 2013). Protoplasts were isolated as described by Yoo et al. (2007), and 50 independent protoplasts were examined for each parameter. Chloroplast size refers to maximal length, and chloroplast surface area and volume were calculated assuming an ellipsoidal shape using the Cesaro formula (Ivanova and P'yankov, 2002), where surface area = $4 \times \pi \times (a \times b^2)^{2/3}$ and volume = $(4/3) \times \pi \times (a \times b^2)$, where a = chloroplast length/2 and b = chloroplast width/2.

Protein Manipulations

Total cell proteins were isolated from Col-0, *im*, *imgi2*, and *gi2* leaves by previously described procedures (Yu et al., 2004) using leaf samples similar to those described above for pigment analyses. In brief, leaves were weighed, frozen in liquid N_2, and homogenized in 2× SDS sample buffer. The homogenates were incubated at 65°C for 2 h, then centrifuged (14,000 rpm for 10 min), and the supernatants were collected and electrophoresed through 12% SDS polyacrylamide gels on an equal fresh weight basis. Western immunoblot analyses were carried out by established protocols using polyclonal antibodies to the large subunit of Rubisco, the light-harvesting complex protein, the α-subunit of ATP synthase, PSII subunit O, PSI subunit F, PSII reaction center protein, and the Rieske Fe-S center of the cytochrome b_6f complex. All of these antibodies have been characterized previously (Yu et al., 2008a). The SuperSignal West Pico chemiluminescence kit (Pierce) was used for signal detection.

Transcript Analysis by Quantitative Reverse Transcription-PCR

Total cell RNAs were isolated from Arabidopsis leaf tissues using the Trizol RNA reagent (Invitrogen), then reverse transcribed using the SuperScript III First-Strand Synthesis System (Invitrogen). The reverse transcription reaction products were diluted 10-fold, and quantitative reverse transcription (qRT)-PCR was then carried out in a total volume of 25 μL using the Maxima SYBR Green qPCR Master Mix (Thermo Scientific). Expression values were normalized to *ACTIN*, and relative expression values were calculated using the equation 2^{dCT}, where dCT (for cycle threshold) = CT (reference gene) − CT (target gene). Primers used in the expression analyses are listed in Supplemental Table S1.

Chlorophyll Fluorescence Measurements

Chlorophyll fluorescence measurements were conducted as described (Baerr et al., 2005) on the top two pairs of rosette leaves from Col-0 and *imgi2* at the same developmental stage (stages I and III, respectively) using a PAM-2500 chlorophyll fluorometer (Heinz Walz). The leaves were dark adapted (15 min) prior to measurement of steady-state light response curves for EP (the redox state of the first electron acceptor of PSII) and for relative linear electron transport rates.

ROS Staining Assays

Procedures to detect O_2^- using NBT (Sigma-Aldrich) have been described by Ramel et al. (2009). In brief, leaves of Col-0, *im*, *imgi2*, and *gi2* were vacuum infiltrated with 3.5 mg mL^{-1} NBT in 10 mM potassium phosphate buffer containing 10 mM NaN_3. After 2 h, the stained leaves were bleached by boiling for 5 min in an ethanol:glycerol:acetic acid solution (3:1:1, v/v/v). The stained leaves were stored in an ethanol:glycerol solution (4:1, v/v).

Procedures to detect H_2O_2 using DAB (Sigma-Aldrich) have been described by Clarke (2009). In brief, Col-0, *im*, *imgi2*, and *gi2* leaves were vacuum infiltrated with a freshly prepared DAB solution (1 mg mL^{-1}; pH 3.8), then immersed in the same solution for approximately 8 h. After staining, the leaves were bleached by boiling for 10 min in 19:1 ethanol:H_2O (v/v) and stored in an ethanol:glycerol (4:1, v/v) solution.

Starch Staining and Quantification

To qualitatively assess starch contents, Col-0, *im*, *imgi2*, and *gi2* plants were removed from soil just prior to bolting and bleached by boiling in 50 mL of 80% (v/v) ethanol for approximately 30 min. The plants were then stained for starch by immersion for 5 min in a solution of Lugol's iodine (1% [w/v] potassium iodide and 0.1% [w/v] iodine). After staining, the plants were destained in distilled, deionized water for approximately 1 h; photographs were taken immediately.

For starch quantification, Col-0, *im*, *imgi2*, and *gi2* plants were removed form the soil just prior to bolting, then weighed, boiled in 50 mL of 80% (v/v) ethanol, and ground to a slurry using a mortar and pestle. The slurries were centrifuged (8,500 rpm for 10 min), and the pellets were washed twice with 80% ethanol, resuspended in 15 mL of distilled, deionized water, and boiled for 30 min. Total starch content was quantified using a Glc assay kit (R-Biopharm) according to the manufacturer's instructions.

CO_2 Assimilation Measurements

A LI-COR 6400 (Li-Cor) was used to measure CO_2 assimilation rates with respect to the internal CO_2 concentration. The CO_2 assimilation rate-internal CO_2 concentration curves were plotted at a photosynthetic photon flux density of 200 μmol m^{-2} s^{-1}, and the reference and sample infrared gas analyzers were matched automatically before taking each measurement.

Sequence data from this article can be found in the GenBank/EMBL data libraries under accession numbers At4g22260, NC_003075.7; At1g22770, NC_003070.9; At3g11540, NC_003074.8; and At1g10760, NC_003070.9.

Supplemental Data

The following materials are available in the online version of this article.

Supplemental Table S1. Primers used in this study.

Received September 19, 2014; accepted October 15, 2014; published October 27, 2014.

LITERATURE CITED

Albrecht M, Klein A, Hugueney P, Sandmann G, Kuntz M (1995) Molecular cloning and functional expression in *E. coli* of a novel plant enzyme mediating ζ-carotene desaturation. FEBS Lett **372:** 199–202

Aluru MR, Bae H, Wu D, Rodermel SR (2001) The Arabidopsis *immutans* mutation affects plastid differentiation and the morphogenesis of white and green sectors in variegated plants. Plant Physiol **127:** 67–77

Aluru MR, Stessman DJ, Spalding MH, Rodermel SR (2007) Alterations in photosynthesis in Arabidopsis lacking IMMUTANS, a chloroplast terminal oxidase. Photosynth Res **91:** 11–23

Baerr JN, Thomas JD, Taylor BG, Rodermel SR, Gray GR (2005) Differential photosynthetic compensatory mechanisms exist in the *immutans* mutant of *Arabidopsis thaliana*. Physiol Plant **124:** 390–402

Cao S, Jiang S, Zhang R (2006) The role of GIGANTEA gene in mediating the oxidative stress response and in Arabidopsis. Plant Growth Regul **48:** 261–270

Cao S, Song YQ, Su L (2007) Freezing sensitivity in the gigantea mutant of Arabidopsis is associated with sugar deficiency. Biol Plant **51:** 359–362

Carol P, Stevenson D, Bisanz C, Breitenbach J, Sandmann G, Mache R, Coupland G, Kuntz M (1999) Mutations in the *Arabidopsis* gene *IMMUTANS* cause a variegated phenotype by inactivating a chloroplast terminal oxidase associated with phytoene desaturation. Plant Cell **11:** 57–68

Chory J, Reinecke D, Sim S, Washburn T, Brenner M (1994) A role for cytokinins in de-etiolation in Arabidopsis: *det* mutants have an altered response to cytokinins. Plant Physiol **104:** 339–347

Clarke JD (2009) Phenotypic analysis of Arabidopsis mutants: diaminobenzidine stain for hydrogen peroxide. Cold Spring Harb Protoc **6:** pdb-prot4981

Cortleven A, Nitschke S, Klaumünzer M, Abdelgawad H, Asard H, Grimm B, Riefler M, Schmülling T (2014) A novel protective function for cytokinin in the light stress response is mediated by the ARABIDOPSIS HISTIDINE KINASE2 and ARABIDOPSIS HISTIDINE KINASE3 receptors. Plant Physiol **164:** 1470–1483

Dietz KJ, Schreiber U, Heber U (1985) The relationship between the redox state of Q_A and photosynthesis in leaves at various carbon-dioxide, oxygen and light regimes. Planta **166:** 219–226

Eimert K, Wang SM, Lue WI, Chen J (1995) Monogenic recessive mutations causing both late floral initiation and excess starch accumulation in *Arabidopsis*. Plant Cell **7:** 1703–1712

Fleishon S, Shani E, Ori N, Weiss D (2011) Negative reciprocal interactions between gibberellin and cytokinin in tomato. New Phytol **190:** 609–617

Foudree A, Putarjunan A, Kambakam S, Nolan T, Fussell J, Pogorelko G, Rodermel S (2012) The mechanism of variegation in *immutans* provides insight into chloroplast biogenesis. Front Plant Sci **3:** 260

Fowler S, Lee K, Onouchi H, Samach A, Richardson K, Morris B, Coupland G, Putterill J (1999) GIGANTEA: a circadian clock-controlled gene that regulates photoperiodic flowering in Arabidopsis and encodes a protein with several possible membrane-spanning domains. EMBO J **18:** 4679–4688

Fu A, Liu H, Yu F, Kambakam S, Luan S, Rodermel S (2012) Alternative oxidases (AOX1a and AOX2) can functionally substitute for plastid terminal oxidase in *Arabidopsis* chloroplasts. Plant Cell **24:** 1579–1595

Giacomelli L, Masi A, Ripoll DR, Lee MJ, van Wijk KJ (2007) *Arabidopsis thaliana* deficient in two chloroplast ascorbate peroxidases shows accelerated light-induced necrosis when levels of cellular ascorbate are low. Plant Mol Biol **65:** 627–644

Glynn JM, Froehlich JE, Osteryoung KW (2008) *Arabidopsis* ARC6 coordinates the division machineries of the inner and outer chloroplast membranes through interaction with PDV2 in the intermembrane space. Plant Cell **20:** 2460–2470

Greenboim-Wainberg Y, Maymon I, Borochov R, Alvarez J, Olszewski N, Ori N, Eshed Y, Weiss D (2005) Cross talk between gibberellin and cytokinin: the *Arabidopsis* GA response inhibitor SPINDLY plays a positive role in cytokinin signaling. Plant Cell **17:** 92–102

Grevelding C, Suter-Crazzolara C, von Menges A, Kemper E, Masterson R, Schell J, Reiss B (1996) Characterisation of a new allele of pale cress and its role in greening in Arabidopsis thaliana. Mol Gen Genet **251:** 532–541

Holding DR, Springer PS, Coomber SA (2000) The chloroplast and leaf developmental mutant, pale cress, exhibits light-conditional severity and symptoms characteristic of its ABA deficiency. Ann Bot (Lond) **86:** 953–962

Horner HT, Wagner BL (1980) The association of druse crystals with the developing stomium of *Capsicum annum* (Solanaceae) anthers. Am J Bot **67:** 1347–1360

Hüner NPA, Oquist G, Sarhan F (1998) Energy balance and acclimation to light and cold. Trends Plant Sci **3:** 224–230

Huq E, Tepperman JM, Quail PH (2000) GIGANTEA is a nuclear protein involved in phytochrome signaling in Arabidopsis. Proc Natl Acad Sci USA **97:** 9789–9794

Hutchison CE, Kieber JJ (2002) Cytokinin signaling in *Arabidopsis*. Plant Cell (Suppl) **14:** S47–S59

Itoh H, Izawa T (2011) A study of phytohormone biosynthetic gene expression using a circadian clock-related mutant in rice. Plant Signal Behav **6:** 1932–1936

Ivanov AG, Rosso D, Savitch LV, Stachula P, Rosembert M, Oquist G, Hurry V, Hüner NPA (2012) Implications of alternative electron sinks in increased resistance of PSII and PSI photochemistry to high light stress in cold-acclimated *Arabidopsis thaliana*. Photosynth Res **113:** 191–206

Ivanova LA, P'yankov VI (2002) Structural adaptation of the leaf mesophyll to shading. Russ J Plant Physiol **49:** 419–431

Jacobsen SE, Binkowski KA, Olszewski NE (1996) SPINDLY, a tetratricopeptide repeat protein involved in gibberellin signal transduction in Arabidopsis. Proc Natl Acad Sci USA **93:** 9292–9296

Jacobsen SE, Olszewski NE (1993) Mutations at the *SPINDLY* locus of *Arabidopsis* alter gibberellin signal transduction. Plant Cell **5:** 887–896

Kim WY, Fujiwara S, Suh SS, Kim J, Kim Y, Han L, David K, Putterill J, Nam HG, Somers DE (2007) ZEITLUPE is a circadian photoreceptor stabilized by GIGANTEA in blue light. Nature **449:** 356–360

Koornneef M, Alonso-Blanco C, Blankestijn-de Vries H, Hanhart CJ, Peeters AJ (1998) Genetic interactions among late-flowering mutants of Arabidopsis. Genetics **148:** 885–892

Kurepa J, Smalle J, Van Montagu M, Inzé D (1998a) Oxidative stress tolerance and longevity in Arabidopsis: the late-flowering mutant gigantea is tolerant to paraquat. Plant J **14:** 759–764

Kurepa J, Smalle J, Van Montagu M, Inzé D (1998b) Effects of sucrose supply on growth and paraquat tolerance of the late-flowering *gi-3* mutant. Plant Growth Regul **26:** 91–96

Kusnetsov VV, Oelmüller R, Sarwat M, Porfirova SA, Cherepneva GN, Herrmann RG, Kulaeva ON (1994) Cytokinins, abscisic acid and light affect accumulation of chloroplast proteins in Lupinus luteus cotyledons, without notable effect on steady-state mRNA levels. Planta **194:** 318–327

Lerbs S, Lerbs W, Klyachko NL, Romanko EG, Kulaeva ON, Wollgiehn R, Parthier B (1984) Gene expression in cytokinin- and light-mediated plastogenesis of Cucurbita cotyledons: ribulose-1,5-bisphosphate carboxylase/oxygenase. Planta **162:** 289–298

Levy YY, Dean C (1998) The transition to flowering. Plant Cell **10:** 1973–1990

Li Y, Ren B, Ding L, Shen Q, Peng S, Guo S (2013) Does chloroplast size influence photosynthetic nitrogen use efficiency? PLoS ONE **8:** e62036

Lichtenthaler HK (1987) Chlorophylls and carotenoids: pigments of photosynthetic biomembranes. Methods Enzymol **148:** 350–382

Lichtenthaler HK, Buschmann C (1978) Control of chloroplast development by red light, blue light and phytohormones. *In* G Akoyunoglou, ed, Chloroplast Development. Elsevier, Amsterdam, pp 801–816

Liu X, Yu F, Rodermel S (2010) Arabidopsis chloroplast FtsH, *var2* and suppressors of *var2* leaf variegation: a review. J Integr Plant Biol **52:** 750–761

Matsoukas IG, Massiah AJ, Thomas B (2013) Starch metabolism and antiflorigenic signals modulate the juvenile-to-adult phase transition in *Arabidopsis*. Plant Cell Environ **36:** 1802–1811

McCabe MS, Garratt LC, Schepers F, Jordi WJRM, Stoopen GM, Davelaar E, van Rhijn JHA, Power JB, Davey MR (2001) Effects of P(SAG12)-*IPT* gene expression on development and senescence in transgenic lettuce. Plant Physiol **127:** 505–516

McDonald AE, Ivanov AG, Bode R, Maxwell DP, Rodermel SR, Hüner NPA (2011) Flexibility in photosynthetic electron transport: the physiological role of plastoquinol terminal oxidase (PTOX). Biochim Biophys Acta **1807:** 954–967

Meurer J, Grevelding C, Westhoff P, Reiss B (1998) The PAC protein affects the maturation of specific chloroplast mRNAs in Arabidopsis thaliana. Mol Gen Genet **258:** 342–351

Miyagishima SY, Froehlich JE, Osteryoung KW (2006) PDV1 and PDV2 mediate recruitment of the dynamin-related protein ARC5 to the plastid division site. Plant Cell **18:** 2517–2530

Miyawaki K, Matsumoto-Kitano M, Kakimoto T (2004) Expression of cytokinin biosynthetic isopentenyltransferase genes in Arabidopsis: tissue specificity and regulation by auxin, cytokinin, and nitrate. Plant J **37:** 128–138

Okazaki K, Kabeya Y, Suzuki K, Mori T, Ichikawa T, Matsui M, Nakanishi H, Miyagishima SY (2009) The PLASTID DIVISION1 and 2 components of the chloroplast division machinery determine the rate of chloroplast division in land plant cell differentiation. Plant Cell **21:** 1769–1780

Okegawa Y, Kobayashi Y, Shikanai T (2010) Physiological links among alternative electron transport pathways that reduce and oxidize plastoquinone in Arabidopsis. Plant J **63:** 458–468

Paparelli E, Parlanti S, Gonzali S, Novi G, Mariotti L, Ceccarelli N, van Dongen JT, Kölling K, Zeeman SC, Perata P (2013) Nighttime sugar starvation orchestrates gibberellin biosynthesis and plant growth in *Arabidopsis*. Plant Cell **25:** 3760–3769

Park DH, Somers DE, Kim YS, Choy YH, Lim HK, Soh MS, Kim HJ, Kay SA, Nam HG (1999) Control of circadian rhythms and photoperiodic flowering by the Arabidopsis GIGANTEA gene. Science **285:** 1579–1582

Parthier B (1979) The role of phytohormones (cytokinins) in chloroplast development. Biochem Physiol Pflanz **174:** 173–214

Peltier G, Cournac L (2002) Chlororespiration. Annu Rev Plant Biol **53:** 523–550

Pinhero RG, Rao MV, Paliyath G, Murr DP, Fletcher RA (1997) Changes in activities of antioxidant enzymes and their relationship to genetic and paclobutrazol-induced chilling tolerance of maize seedlings. Plant Physiol **114:** 695–704

Pogany M, Koehl J, Heiser I, Elstner E, Barna B (2004) Juvenility of tobacco induced by cytokinin gene introduction decreases susceptibility to

Tobacco necrosis virus and confers tolerance to oxidative stress. Physiol Mol Plant Pathol **65:** 39–47

Pogson BJ, Albrecht V (2011) Genetic dissection of chloroplast biogenesis and development: an overview. Plant Physiol **155:** 1545–1551

Preston C (1994) Mechanisms of resistance to herbicides interacting with photosystem I. *In* SB Powles, JAM Holtum, eds, Herbicide Resistance in Plants: Biology and Biochemistry. Lewis Publishers, Chelsea, MI, p 61

Putarjunan A, Liu X, Nolan T, Yu F, Rodermel S (2013) Understanding chloroplast biogenesis using second-site suppressors of *immutans* and *var2*. Photosynth Res **116:** 437–453

Ramel F, Sulmon C, Bogard M, Couée I, Gouesbet G (2009) Differential patterns of reactive oxygen species and antioxidative mechanisms during atrazine injury and sucrose-induced tolerance in Arabidopsis thaliana plantlets. BMC Plant Biol **9:** 28

Rédei GP (1962) Supervital mutants of Arabidopsis. Genetics **47:** 443–460

Rédei GP (1963) Somatic instability caused by a cysteine-sensitive gene in Arabidopsis. Science **139:** 767–769

Rédei GP (1967) Biochemical aspects of a genetically determined variegation in Arabidopsis. Genetics **56:** 431–443

Röbbelen G (1968) Genbedingte Rotlicht-Empfindlichkeit der Chloroplasten differenzierung bei *Arabidopsis.* Planta **80:** 237–254

Rosso D, Bode R, Li W, Krol M, Saccon D, Wang S, Schillaci LA, Rodermel SR, Maxwell DP, Hüner NP (2009) Photosynthetic redox imbalance governs leaf sectoring in the *Arabidopsis thaliana* variegation mutants *immutans*, *spotty*, *var1*, and *var2*. Plant Cell **21:** 3473–3492

Rosso D, Ivanov AG, Fu A, Geisler-Lee J, Hendrickson L, Geisler M, Stewart G, Krol M, Hurry V, Rodermel SR, et al (2006) IMMUTANS does not act as a stress-induced safety valve in the protection of the photosynthetic apparatus of Arabidopsis during steady-state photosynthesis. Plant Physiol **142:** 574–585

Sakakibara H (2006) Cytokinins: activity, biosynthesis, and translocation. Annu Rev Plant Biol **57:** 431–449

Sawa M, Kay SA (2011) GIGANTEA directly activates Flowering Locus T in *Arabidopsis thaliana*. Proc Natl Acad Sci USA **108:** 11698–11703

Sawa M, Nusinow DA, Kay SA, Imaizumi T (2007) FKF1 and GIGANTEA complex formation is required for day-length measurement in *Arabidopsis*. Science **318:** 261–265

Shahbazi M, Gilbert M, Labouré AM, Kuntz M (2007) Dual role of the plastid terminal oxidase in tomato. Plant Physiol **145:** 691–702

Shigeoka S, Ishikawa T, Tamoi M, Miyagawa Y, Takeda T, Yabuta Y, Yoshimura K (2002) Regulation and function of ascorbate peroxidase isoenzymes. J Exp Bot **53:** 1305–1319

Slade P (1966) The fate of paraquat applied to plants. Weed Res **6:** 158–167

Smith WK, Vogelmann TC, DeLucia EH, Bell DT, Shepherd KA (1997) Leaf form and photosynthesis: do leaf structure and orientation interact to regulate internal light and carbon dioxide? BioScience **47:** 785–793

Stoynova EZ, Iliev LK, Georgiev GT (1996) Structural and functional alterations in radish plants induced by the phenylurea cytokinin 4-PU-30. Biol Plant **38:** 237–244

Sun CW, Chen LJ, Lin LC, Li HM (2001) Leaf-specific upregulation of chloroplast translocon genes by a CCT motif-containing protein, CIA 2. Plant Cell **13:** 2053–2061

Swain SM, Tseng TS, Olszewski NE (2001) Altered expression of *SPINDLY* affects gibberellin response and plant development. Plant Physiol **126:** 1174–1185

Tseng TS, Salomé PA, McClung CR, Olszewski NE (2004) SPINDLY and GIGANTEA interact and act in *Arabidopsis thaliana* pathways involved in light responses, flowering, and rhythms in cotyledon movements. Plant Cell **16:** 1550–1563

van der Graaff E, Hooykaas P, Lein W, Lerchl J, Kunze G, Sonnewald U, Boldt R (2004) Molecular analysis of "de novo" purine biosynthesis in solanaceous species and in Arabidopsis thaliana. Front Biosci **9:** 1803–1816

Wang J, Letham DS, Cornish E, Wei K, Hocart CH, Michael M, Stevenson KR (1997) Studies of cytokinin action and metabolism using tobacco plants expressing either the *ipt* or the GUS gene controlled by a chalcone synthase promoter *ipt* and GUS gene expression, cytokinin levels and metabolism. Aust J Plant Physiol **24:** 673–683

Wang TL, Thompson AG, Horgan R (1977) A cytokinin glucoside from the leaves of Phaseolus vulgaris L. Planta **135:** 285–288

Werner T, Motyka V, Laucou V, Smets R, Van Onckelen H, Schmülling T (2003) Cytokinin-deficient transgenic *Arabidopsis* plants show multiple developmental alterations indicating opposite functions of cytokinins in the regulation of shoot and root meristem activity. Plant Cell **15:** 2532–2550

Wetzel CM, Jiang CZ, Meehan LJ, Voytas DF, Rodermel SR (1994) Nuclear-organelle interactions: the *immutans* variegation mutant of Arabidopsis is plastid autonomous and impaired in carotenoid biosynthesis. Plant J **6:** 161–175

Woo NS, Gordon MJ, Graham SR, Rossel JB, Badger MR, Pogson BJ (2011) A mutation in the purine biosynthetic enzyme ATASE2 impacts high light signalling and acclimation response in green and chlorotic sectors of Arabidopsis leaves. Funct Plant Biol **38:** 401–419

Wu D, Wright DA, Wetzel C, Voytas DF, Rodermel S (1999) The *IMMUTANS* variegation locus of *Arabidopsis* defines a mitochondrial alternative oxidase homolog that functions during early chloroplast biogenesis. Plant Cell **11:** 43–55

Yano R, Nakamura M, Yoneyama T, Nishida I (2005) Starch-related α-glucan/water dikinase is involved in the cold-induced development of freezing tolerance in Arabidopsis. Plant Physiol **138:** 837–846

Yaronskaya E, Vershilovskaya I, Poers Y, Alawady AE, Averina N, Grimm B (2006) Cytokinin effects on tetrapyrrole biosynthesis and photosynthetic activity in barley seedlings. Planta **224:** 700–709

Yoo SD, Cho YH, Sheen J (2007) Arabidopsis mesophyll protoplasts: a versatile cell system for transient gene expression analysis. Nat Protoc **2:** 1565–1572

Yu F, Fu A, Aluru M, Park S, Xu Y, Liu H, Liu X, Foudree A, Nambogga M, Rodermel S (2007) Variegation mutants and mechanisms of chloroplast biogenesis. Plant Cell Environ **30:** 350–365

Yu F, Liu X, Alsheikh M, Park S, Rodermel S (2008a) Mutations in *SUPPRESSOR OF VARIEGATION1*, a factor required for normal chloroplast translation, suppress *var2*-mediated leaf variegation in *Arabidopsis*. Plant Cell **20:** 1786–1804

Yu F, Park S, Rodermel SR (2004) The Arabidopsis FtsH metalloprotease gene family: interchangeability of subunits in chloroplast oligomeric complexes. Plant J **37:** 864–876

Yu JW, Rubio V, Lee NY, Bai S, Lee SY, Kim SS, Liu L, Zhang Y, Irigoyen ML, Sullivan JA, et al (2008b) COP1 and ELF3 control circadian function and photoperiodic flowering by regulating GI stability. Mol Cell **32:** 617–630

Yu TS, Kofler H, Häusler RE, Hille D, Flügge UI, Zeeman SC, Smith AM, Kossmann J, Lloyd J, Ritte G, et al (2001) The *Arabidopsis sex1* mutant is defective in the R1 protein, a general regulator of starch degradation in plants, and not in the chloroplast hexose transporter. Plant Cell **13:** 1907–1918

Zavaleta-Mancera HA, Thomas BJ, Thomas H, Scott IM (1999) Regreening of senescent Nicotiana leaves. II. Redifferentiation of plastids. J Exp Bot **50:** 1683–1689